SENSOR LETTERS
Vol. 3, 274–295, 2005

REVIEW

Humidity Sensors: A Review of Materials and Mechanisms

Zhi Chen* and Chi Lu

Department of Electrical and Computer Engineering and Center for Nanoscale Science and Engineering, University of Kentucky, Lexington, Kentucky 40506, USA

(Received: 22 July 2005. Accepted: 27 July 2005)

We have reviewed humidity sensors based on various materials for both relative and absolute humidity, including ceramic, semiconducting, and polymer materials. In the majority of publications, there are few papers dealing with absolute humidity sensors, which have extensive applications in industry. We reviewed extensively absolute humidity sensors in this article, which is unique comparing with other reviews of humidity sensors. The electrical properties of humidity sensors such as sensitivity, response time, and stability have been described in details for various materials and a considerable part of the review is focused on the sensing mechanisms. In addition, preparation and characterization of sensing materials are also described. For absolute humidity sensors, mirror-based dew-point sensors and solid-state Al_2O_3 moisture sensors have been described. As the major problem in Al_2O_3 moisture sensors, long-term instability, has been solved, α-Al_2O_3 moisture sensors may have promising future in industry.

Keywords: Humidity Sensor, Mechanisms, Humidity-Sensing, Relative Humidity, Absolute Humidity, Dew Point, Frost Point.

CONTENTS

1. Introduction 274
2. Classification of Humidity Sensors 275
3. Relative Humidity Sensors 275
3.1. Ceramic Sensing Materials 275
3.2. Semiconducting Sensing Materials 280
3.3. Polymer-Based Humidity Sensors 281
4. Absolute Humidity Sensors (Hygrometers) 286
4.1. Mirror-Based Dew/Frost Point Sensors (Hygrometers) . . . 286
4.2. Aluminum Oxide Moisture Sensors 289
5. Conclusions 292
References and Notes 292

1. INTRODUCTION

Humidity sensors have gained increasing applications in industrial processing and environmental control.[1] For manufacturing highly sophisticated integrated circuits in semiconductor industry, humidity or moisture levels are constantly monitored in wafer processing. There are many domestic applications, such as intelligent control of the living environment in buildings, cooking control for microwave ovens, and intelligent control of laundry etc. In automobile industry, humidity sensors are used in rear-window defoggers and motor assembly lines. In medical field, humidity sensors are used in respiratory equipment, sterilizers, incubators, pharmaceutical processing, and biological products. In agriculture, humidity sensors are used for green-house air-conditioning, plantation protection (dew prevention), soil moisture monitoring, and cereal storage. In general industry, humidity sensors are used for humidity control in chemical gas purification, dryers, ovens, film desiccation, paper and textile production, and food processing.

In this paper, we aim to present extensive review of research and development of humidity sensors for a wide variety of applications. Because applications in each field require different operating conditions, various types of humidity sensors based on a variety of sensing materials will be described. This paper is organized as follows. It begins with brief review of classification of humidity sensors based on types of sensing materials and detection ranges (Section 2). Then the relative humidity sensors based on ceramic, semiconductor, and polymer materials will be discussed in Section 3. Absolute humidity sensors, which were not extensive studied but are found

*Corresponding author; E-mail: zhichen@engr.uky.edu

 1546-198X/2005/3/274/022 doi:10.1166/sl.2005.045

wide-spread applications in many industrial fields, will be reviewed in Section 4.

2. CLASSIFICATION OF HUMIDITY SENSORS

Humidity measurement determines the amount of water vapor present in a gas that can be a mixture, such as air, or a pure gas, such as nitrogen or argon. Based on measurement techniques, the most commonly used units for humidity measurement are Relative Humidity (RH), Dew/Frost point (D/F PT) and Parts Per Million (PPM).[2] Relative Humidity (RH) is the ratio of the partial pressure of water vapor present in a gas to the saturation vapor pressure of the gas at a given temperature. RH is a function of temperature, and thus it is a relative measurement. The RH measurement is expressed as a percentage. Dew point is the temperature (above 0 °C) at which the water vapor in a gas condenses to liquid water. Frost point is the temperature (below 0 °C) at which the vapor condenses to ice. D/F PT is a function of the pressure of the gas but is independent of temperature and is therefore defined as absolute humidity measurement. Parts Per Million (PPM) represents water vapor content by volume fraction (PPMv) or, if multiplied by the ratio of the molecular weight of water to that of air, as PPMw. PPM is also an absolute measurement. Although this measurement unit is more difficult to conceive, it has extensive applications in industry especially for trace moisture measurement.

Figure 1 shows the correlation among Relative Humidity (RH), Parts Per Million by volume (PPMv), and the Dew/Frost Point (D/F PT). RH measurement covers higher humidity range, PPMv covers lower humidity range, and

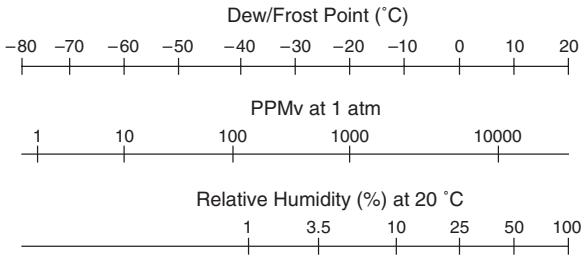

Fig. 1. Correlation among humidity units: Relative Humidity (RH), Dew/Frost point (D/F PT), and Parts Per Million by volume fraction (PPMv).

D/F PT covers all the humidity range. Therefore, for daily life, Relative Humidity is constantly used for ease understanding. For trace moisture measurement, it would better to use PPMv or D/F PT, because it tells us the absolute amount of water vapor in a gas or air. According to the measurement units, humidity sensors are divided into two types: Relative humidity (RH) sensors and absolute humidity (moisture) sensors. Most humidity sensors are relative humidity sensors, which can be further classified into ceramic, semiconductor, and polymer humidity sensors. Two types of absolute humidity sensors or hygrometers are available, including solid moisture sensor and mirror-chilled hygrometer.

3. RELATIVE HUMIDITY SENSORS

3.1. Ceramic Sensing Materials

Humidity sensors based on water-phase protonic ceramic materials are used widely in industry and research laboratories. The adsorbed water condensed on the surface of

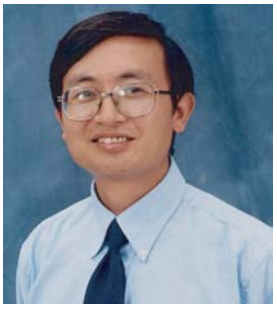

Zhi Chen received his B.S. degree in 1984 and M.S. degree in 1987 in electrical engineering from University of Electronic Science and Technology, Chengdu, China. He obtained a Ph.D. degree in electrical engineering from University of Illinois at Urbana-Champaign in 1999. He is currently an associate professor with Department of Electrical Engineering and the associate director of Center for Nanoscale Science and Engineering, University of Kentucky. He is a senior member of IEEE and won the National Science Foundation CAREER Award in 2001. His research interests include micro/nano fabrication, nanoscale devices and materials including growth of highly ordered carbon nanotubes for electronic device applications, CMOS transistor reliability and deuterium processing, gate dielectrics for MOS transistors, and microsensors.

Chi Lu received his B.S. degree in Environmental Engineering from Hebei University of Science and Technology, China in 1996 and M.S. degree in Materials Science from Beijing University of Chemical Technology, China in 1999. He is currently a Ph.D. student at Department of Electrical Engineering, University of Kentucky. His research interests include gas sensors and nanodevices.

REVIEW

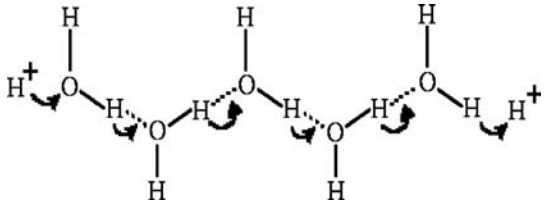

Fig. 2. Brief illustration of the Grotthuss mechanism.

the materials and protons will be conducted in the formed aquatic layers. For ionic sensing materials, if the humidity increases, the conductivity decreases and the dielectric constant increases.[3,4] In bulk water, proton is the dominant carrier responsible for the electrical conductivity. The conduction is due to the Grotthuss mechanism, through which protons tunnel from one water molecule to the next via hydrogen bonding that universally exists in liquid-phase water (Fig. 2).

This mechanism was reported about 200 years ago.[5] The mechanism of protonic conduction inside the adsorbed water layers on the surface of the sensing materials was discovered in study of TiO_2 and α-Fe_2O_3.[6,7] As shown in Figure 3, at the first stage of adsorption, a water molecule is chemically adsorbed on an activated site (a) to form an adsorption complex (b), which subsequently transfers to surface hydroxyl groups (c). Then, another water molecule comes to be adsorbed through hydrogen bonding on the two neighboring hydroxyl groups as shown in (d). The top water molecule condensed cannot move freely due to the restriction from the two hydrogen bonding (Fig. 3(d)). Thus this layer or the first physically-adsorbed layer is immobile and there are not hydrogen bonds formed between the water molecules in this layer. Therefore, no proton could be conducted in this stage.

As water continues to condense on the surface of the ceramic, an extra layer on top of the first physically-adsorbed layer forms (Fig. 4). This layer is less ordered than the first physically-adsorbed. For example, there may be only one hydrogen bond locally. If more layers

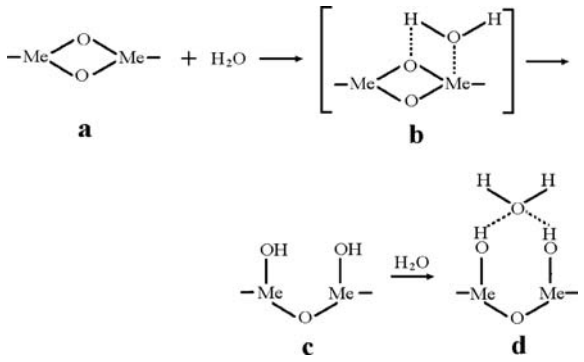

Fig. 3. Four stages of the adsorption. Reprinted with permission from [6], T. Moromoto et al., *J. Phys. Chem.* 73, 243 (**1969**). © 1969, American Chemical Society.

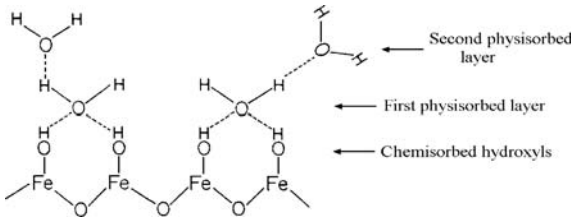

Fig. 4. Multi-layer structure of condensed water. Reprinted with permission from [7], E. McCafferty et al., *Faraday Discussions* 52, 239 (**1971**). © 1971, Royal Society of Chemistry.

condense, the ordering from the initial surface may gradually disappear and protons may have more and more freedom to move inside the condensed water through the Grotthuss mechanism. In other words, from the second physisorbed layer, water molecules become mobile and finally almost identical to the bulk liquid water, and the Grotthuss mechanism becomes dominant. This mechanism indicates that sensors based purely on water-phase protonic conduction would not be quite sensitive to low humidity, at which the water vapor could rarely form continuous mobile layers on the sensor surface.

The two immobile layers, the chemisorbed and the first physisorbed ones, while cannot contribute to proton-conducting activity, could provide electron tunnelling between donor water sites.[8,9] The tunnelling effect, along with the energy induced by the surface anions, facilitates electrons to hop along the surface that is covered by the immobile layers and therefore contributes to the conductivity. This mechanism is quite helpful for detecting low humidity levels, at which there is not effective protonic conduction. Nonetheless, the tunnelling effect is definitely not the semiconducting mechanism that will be discussed later.

In the following subsections, we will describe four basic types of oxide-based sensing materials, including Al_2O_3, TiO_2, SiO_2, and spinel compounds. The basic preparation methods, humidity-sensing properties, and their advantages and disadvantages will be discussed in detail.

3.1.1. Al_2O_3

Al_2O_3 is one of the most favorable ceramic sensing materials due to its independence of temperature at nearly all range of relative humidity from 25 °C to 80 °C.[10] The small pore radius makes Al_2O_3 sensitive to very low water vapor pressure. Due to the electron tunnelling effect inside the condensed immobile water layers, porous Al_2O_3 is a competitive candidate for sensing low humidity levels.[8] In addition to capacitive and resistive sensors, more complicated sensing devices based on Al_2O_3, e.g., MISFETs (metal-insulator-semiconductor field-effect transistors), were fabricated, and some of them have very good linear response.[11]

There are several phases for Al_2O_3 whereas only two of them are common and used in humidity sensing: γ-Al_2O_3

(amorphous) and α-Al_2O_3 (corundum). The former is more sensitive than the latter due to its high porosity, while the latter is most thermodynamically stable phase. Although many Al_2O_3-based humidity sensing applications use the γ-phase or amorphous phase Al_2O_3, the films are susceptible to change to γ-$Al_2O_3 \cdot H_2O$ (boehmite),[12] resulting in the gradual decrease of surface area and porosity.[13] Therefore the deposition or growth of humidity-sensitive (porous) α-Al_2O_3 is also important for sensors required for long-term, non-regenerate applications. Because γ-Al_2O_3 is always mixed with huge amount of amorphous Al_2O_3, the crystal content is quite small and amorphous Al_2O_3 formed by anodization or vacuum deposition contains γ-phase to some degree, whereas the former is crystalline and the latter has no significant peaks in X-ray diffraction except for one broad peak.

Many of the present Al_2O_3 humidity sensors are fabricated through anodization. Because of its low-cost and easy process, anodic Al_2O_3 has great priority over other ceramics. The anodization technique can be divided into two categories, low voltage ($<$100 V) anodization and anodic spark deposition (usually $>$100 V). The low voltage anodization produces γ-phase or amorphous Al_2O_3 and the anodic spark deposition results in porous α-Al_2O_3. These two methods will be discussed first and other methods for fabrication of humidity-sensing Al_2O_3 will be discussed later.

The first humidity-sensitive Al_2O_3 layer formed through anodization on Al metal surface was reported in 1953.[4] The anodization was carried out in 3% H_2CrO_3 at 50 V. The capacitance increased linearly while resistance decreased exponentially to the relative humidity, both of the capacitive and resistive sensitivities are considerably affected by the temperature. The anodization parameters considerably affected the moisture sensitivity of the resulted porous Al_2O_3 films. As reported in Refs. [14, 15], the capacitance/ resistance versus humidity characteristic of the sensor fabricated at low current density shows a weak response at low humidity, whereas for anodization at high current density or re-anodization a much steeper response at low humidity is obtained. This phenomenon has been attributed to trapping of anions of electrolytes at high current density or into the pores by re-anodization. The high charge density results in easy physisorption of water molecules that form a liquid-like network within the pores (as discussed in the previous section).

The primary problem of anodized amorphous Al_2O_3 as discussed before is that when exposed for a long duration in high humidity, significant degradation in the sensitivity and drift in the capacitance characteristics would be expected. This was attributed to the widening of the pores due to diffusion of the adsorbed water.[16] The best solution would be to grow self-ordered porous films and eliminating the variability among the pores and irregularities the microstructure of the film. Thermal annealing at about 400 °C has been reported to have limited improvement of the stability of anodized Al_2O_3 sensors.[17]

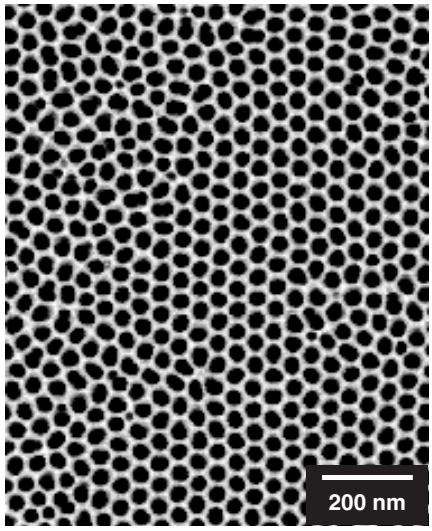

Fig. 5. Honeycomb structure of anodic aluminum oxide (AAO).

Although amorphous AAO (anodic aluminum oxide) was found to be humidity-sensitive in 1950s, it was not until 1978 did the researchers discover that it could form regular microstructure.[18] Low voltage anodization at certain conditions (always characterized by long-term anodization period at a constant voltage) in acidic electrolyte solution forms Al_2O_3 layer consisting of hexagonal close-packed cylindrical pores perpendicular to the metal surface (Fig. 5). The diameters and depths of the pores can be controlled by tuning the anodization conditions. Therefore, the detection limit could be set very low by shrinking the pore size (as mentioned before, the minimum detectable humidity decreases as the pore radius decreases). In addition to its ease process, this honeycomb structure has great potential applications in electronic, optical, and micromechanical devices.[19, 20]

For humidity-sensitive field-effect transistors (HUMI FET),[21] porous Al_2O_3 film is usually sandwiched between a top Au electrode and an under-gate Al electrode. It is also reported that a HUMIFET with a structure of $SiO_2/Si_3N_4/Ta/Ta_2O_5/Al_2O_3$ exhibits much higher sensitivity (less than 1 ppmv) and faster response time (less than 1 second) than conventionally anodized Al_2O_3.[11]

As a high voltage anodization procedure, anodic spark deposition can create porous α-Al_2O_3[22, 23] films ($\sim$10 μm) that would almost not degrade in humid environments.[24, 25] The electrolytes of anodic spark deposition are not water solutions but high-temperature salt melts (usually alkali salts).[23] Due to the tremendous energy dissipated at very large instantaneous current density ($\sim 10^4$ A/cm^2), the already deposited Al_2O_3 barrier film breaks down and electric sparks occur. The extremely high temperature resulted from the electric sparks melt the Al_2O_3 film locally, resulting in a porous structure (Fig. 6).[24] Re-anodization of the porous α-Al_2O_3 in certain acid solutions at a low voltage was found to be effective in increase of the film resistance

REVIEW

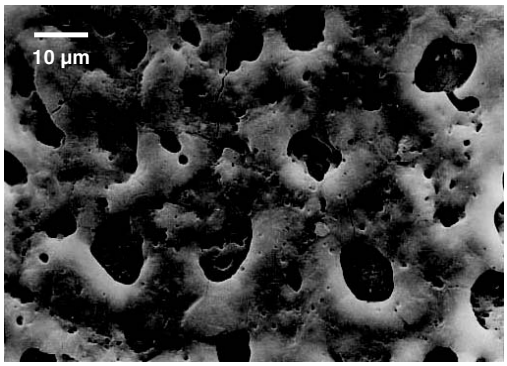

Fig. 6. Porous Al_2O_3 by anodic spark deposition. Reprinted with permission from [24], Z. Chen et al., *J. Am. Ceram. Soc.* 74, 1325 **(1991)**. © 1991, American Ceramic Society.

so that no short-circuit occurs.[24, 25] Figure 7 shows the electrical characteristics of the α-Al_2O_3 sensors versus the relative humidity (RH) at various temperatures.[25] Their response time and long-term stability are also shown in Figures 8 and 9.[25] The α-Al_2O_3 sensors showed very high sensitivity and very fast response at RH range (<5 s). To test its long-term stability, it was exposed in the air for one year and its reading was still the same as its initial one (Fig. 9).

Cathodically grown aluminum hydroxide, or hydrated Al_2O_3, can also be used as a humidity sensing materials.[26] Using electroanalyzing saturated $Al_2(SO_4)_3$ as solution and a hydrogen-adsorbing metal (palladium) as the cathode, aluminum hydroxide film can be deposited on the palladium. Although this film has good response at high humidity, it is not sensitive to low humidity. Electroanalysis is not the only method to fabricate Al_2O_3 thin films.

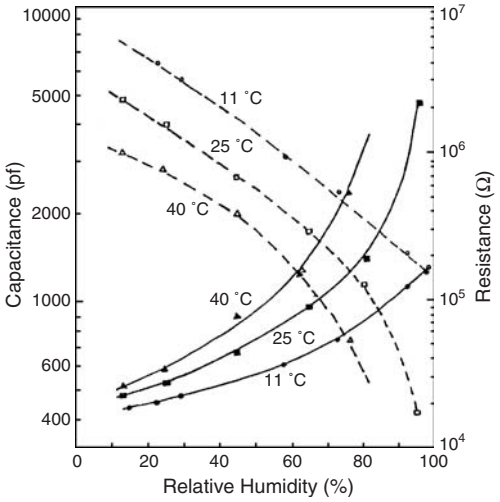

Fig. 7. Capacitance (—) and resistance (- - - -) response of the α-Al_2O_3 sensor to relative humidity at 11 °C, 25 °C, and 40 °C. Reprinted with permission from [25], Z. Chen et al., in *Proc. 27th Annual Conf. IEEE Industry Appl. Soc.*, Houston, TX **(1992)**, Vol. 2, p. 1668. © 1992, IEEE.

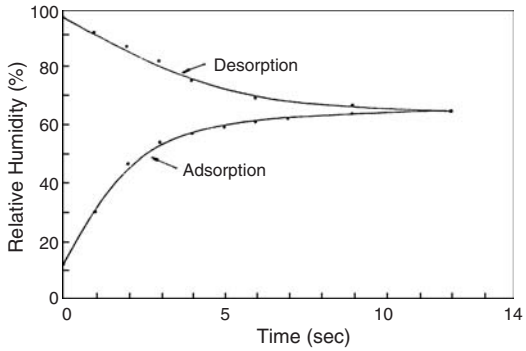

Fig. 8. Time responses of the α-Al_2O_3 sensor to relative humidity from 12 to 65% and from 95% to 65%. Reprinted with permission from [25], Z. Chen et al., in *Proc. 27th Annual Conf. IEEE Industry Appl. Soc.*, Houston, TX **(1992)**, Vol. 2, p. 1668. © 1992, IEEE.

Other methods, such as electron beam evaporation, reactive evaporation, sputtering, spray pyrolysis, etc., were also utilized to deposit Al_2O_3 thin films. Unfortunately, similar to the films formed at low-voltage anodization, Al_2O_3 films prepared by vacuum methods at lower substrate temperatures are usually γ-phase or amorphous, which suffers from degradation as mentioned before. An effective method to obtain porous α-Al_2O_3 (stable) for humidity sensing is reactive evaporation at elevated substrate temperatures (800–1300 °C),[27] in which the metal aluminum is evaporated and oxidized before the oxide particles are deposited on the substrate. Reactively evaporated Al_2O_3 films have been reported to be sensitive to moisture levels as low as 1 ppmv.[28]

Amorphous Al_2O_3 films deposited by spray pyrolysis at 250–350 °C from aluminum acetylacetonate dissolved in dimethyl formamide were found to be humidity-sensitive.[29] However, degradation was not mentioned in the report. Humidity sensors based on bulk-sintered Al_2O_3 films are also reported. However, they are only sensitive to water vapor levels higher than 50–100 ppmv due to the less porosity.[30, 31] The Al_2O_3 sensors for absolute humidity measurement will be described in more detail in Section 4.2.

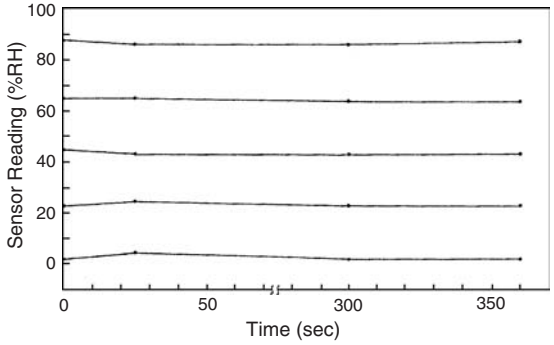

Fig. 9. Long-term stability testing results of the α-Al_2O_3 sensor in the RH range. Reprinted with permission from [25], Z. Chen et al., in *Proc. 27th Annual Conf. IEEE Industry Appl. Soc.*, Houston, TX **(1992)**, Vol. 2, p. 1668. © 1992, IEEE.

3.1.2. TiO_2

TiO_2 has three phases: anatase, rutile, and brookite. The third one is seldom used in humidity sensing. When heated strongly (~1000 °C), anatase automatically transforms to the rutile structure.[32] Rutile is the most common phase of TiO_2, while anatase is very rare in nature. At high temperature (~600 °C), anatase is an *n*-type semiconductor but rutile is a *p*-type one.[33] Their sensing responses to reducing gases like H_2 usually behave on the opposite directions. However, because humidity sensing is usually realized by the adsorbed proton-conducting water layers on the porous structure at room temperature,[7, 34, 35] both phases should behave approximately the same in resistance or capacitance changes. In this section, we will consider TiO_2 as a surface protonic/ionic conducting material, not a semiconducting sensing material.

For humidity sensing applications, anatase TiO_2 are usually made by sol–gel method. The sintering must be at low temperatures (e.g., <500 °C) for short time. Otherwise, TiO_2 may be turned into rutile. Due to its higher water adsorption capacity,[36] anatase is a preferred humidity sensing material. Most commercial TiO_2 powders have rutile phase, which can be fabricated by sputtering, thermal evaporation,[37] pulse laser deposition,[38] and laser molecular-beam epitaxy.[39]

Because of its protonic conducting sensing mechanism, doping with alkali ions may improve the conductivity of TiO_2.[40–42] Adding SnO_2 increases its porosity and thus enhances the sensitivity at high RH range (>70% RH).[43] In addition, bilayered TiO_2/SnO_2,[44] TiO_2/Al-doped ZnO,[45] and ZrO_2/SnO_2[46] were reported to have less hysteresis than pure TiO_2, Al-doped ZnO, and ZrO_2. In these bilayered structures, one material is responsible for fast-adsorption, the other one is responsible for fast-desorption, and porous TiO_2 facilitates the adsorption process of water vapors in the pores. Furthermore, doping of electrolytes or ions, e.g., P_2O_5[47] or potassium[48] may considerably enhance the sensitivity. However, most TiO_2-based sensors using the above fabrication methods are not sensitive at low humidity levels and have limited detection ranges from 10% to 30% RH.[36, 42, 43] A newly developed TiO_2 nanowire sensor is only capable to detect relative humidity levels down to 11%.[49] For K^+-doped TiO_2 film sintered at a temperature below 500 °C, it is capable to sense humidity levels lower than 10%.[48] In addition to resistive/capacitive sensors, sensors based on magneto-elastic method was found to be sensitive to a humidity level of 2% RH,[50] in which the change of mass of TiO_2 (pore size around 80 nm) due to water-adsorption is measured.

3.1.3. SiO_2

Although SiO_2 grown by wet or dry oxidation has been used as an insulator in electronics for a long time, it is definitely not suitable for humidity sensing because it is a dense material. Humidity sensors based on porous silicon oxide were fabricated using bulk-sintering processes, especially traditional sol–gel method, in which SiO_2 is precipitated by hydrolysis of certain alkoxide of silane.[51–53] Nonetheless, the most prominent merit of SiO_2 as a humidity sensing material is its compatibility with the current microelectronics industry. Similar to other porous ceramic materials, the humidity sensitivity of SiO_2 can be enhanced by adding electrolyte dopants, e.g., LiCl.[54] Although it was reported that sol–gel fabricated SiO_2 sensor could detect humidity as low as 4% RH,[51] most reported works showed that only humidity over 20% RH can be detected.[52–54]

During the last few years, humidity sensors based on silicon monoxide (SiO), a powder that is used as a coating material, have been prepared by a novel film fabrication method, glancing angle deposition (GLAD). In this method, the substrate is highly oblique to the incident vapor flux and isolated columns of the material deposited grow toward the vapor source.[55] It is possible to control the film microstructure on a 10 nm scale.[56, 57] Although the SiO films deposited by GLAD are not sensitive to humidity levels lower than 15% RH, the response and recovery times are as short as in milliseconds. These may be the fastest humidity sensors ever reported.

3.1.4. Spinel Compounds

The spinel compounds belong to a large group of oxides with a general composite of AB_2O_4. A can be a divalent metal element, especially in group II, group IIB, and VIIIB. X generally represents a trivalent metal, e.g., iron, chromium, and aluminum. The structure of this group is tetrahedron (diamond) always with high density of defects. Although spinel oxides are semiconductors, most of the reported humidity sensors[58–60] based on these materials have ionic sensing properties probably due to their low operating temperatures (<100 °C). In case that the pore size is very small (100 ~ 300 nm), the lower detection limit can be down to 1% RH.[59, 61] Like other humidity sensing ceramics based on proton-conducting mechanism, doping with alkali ions facilitates formation of hydrated protons.[60] Similar to perovskite oxides, spinel oxides are fabricated by bulk-sintering of the mixture of two metal oxides.[58, 60]

3.1.5. Other Ceramic Sensing Materials

LiCl-doped $MnWO_4$ (a *p*-type semiconductor) prepared by bulk-sintering was reported to have good linear response to relative humidity over 30% RH in short response (~3 s) and recovery (~15 s) time at room temperature.[62, 63] Scanning electron microscopy (SEM) showed different grain and pore sizes of the material in relation to the amount of added LiCl.[64] Despite their short response/recovery time, thin films are less sensitive than thick films due to their lack of capillary structures.[65] Boron phosphate calcinated at 350 °C was found to be sensitive to RH over 35%.[66]

REVIEW

The phosphate cations might dissolve in the adsorbed water and help the formation of protons. α-Fe_2O_3 (hematite) has been used for humidity sensing dated back to the 60's of the last century.[6,7] After doping with silicon and sintering at 850–950 °C, the average pore size of α-Fe_2O_3 is ~25 Å. The α-Fe_2O_3 sensors can response to RH below 5%.[67]

3.2. Semiconducting Sensing Materials

Some ceramic oxides or composite oxides such as SnO_2, ZnO, and In_2O_3, etc. are wide-bandgap semiconductors. H_2O is adsorbed on the oxide surface in molecular and hydroxyl forms. Water molecules are observed to increase the conductivity of *n*-type ceramics and to decrease the conductivity of *p*-type ceramics.[68,69] This effect has been attributed to the donation of electrons from the chemically adsorbed water molecules to the ceramic surface.[68] Another mechanism was proposed.[70,71] It was suggested that water molecules replace the previously adsorbed and ionized oxygen (O^-, O^{2-}, etc.) and therefore release the electrons from the ionized oxygen.[70,71] Probably the "donor effect" could be resulted from both.

Because the conductivity is caused by the surface concentration of electrons, this sensing style is usually called "electronic type." However, the water layer formed by the physical adsorption may be somewhat proton-conductive. Therefore, at room temperatures the conductivity of ceramic semiconducting materials is actually due to addition of both electrons and protons (ionic), unless at high temperatures (>100 °C) moisture cannot effectively condense on the surface. In Figure 10a, the conductivity increment is produced by surface electron accumulation resulting from the preferential alignment of the water dipoles.[68] Hydrogen atoms contact the surface (mostly at the oxygen sites) and attract electrons outward (Fig. 4). In Figure 10b, a depletion region forms originally due to adsorbed oxygen and the released electrons may neutralize the depletion. Since adsorbed water molecules increase the conductivity of *n*-type ceramic semiconductors, nearly all the published works deal with *n*-type ceramics. It was reported that the change of conductivity was linear to certain exponential based on the proposed surface reaction mechanism.[71] However, most of works lack the derivation for establishing strict reaction models.[72]

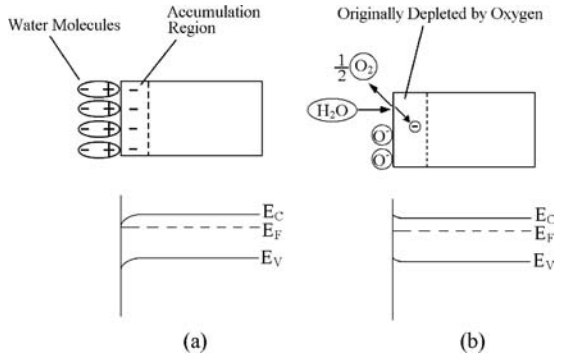

Fig. 10. Two possible mechanisms for the "donor effect" (just for *n*-type): (a) Electrons are attracted by the adsorbed water molecules to the semiconductor surface and the energy bands are bended; (b) Electrons are released by the competitive adsorption.

3.2.1. SnO_2

Stannic oxide (SnO_2) is an *n*-type wide-bandgap semiconductor. H_2O is adsorbed on the oxide surface in molecular and hydroxyl forms and the mechanism was identified to be electronic.[68,72] A more complicated SnO_2–H_2O interaction model was constructed on considering of water desorption in molecular form, dissociative chemisorption and desorption of OH^- groups.[73] The water molecule still behaves like a donor on the SnO_2 surface. Different from TiO_2 and other high-temperature semiconducting ceramics, SnO_2 shows electronic conductivity at rather low temperature (even at room temperatures).[68,70,72,73] Therefore, SnO_2 humidity sensors based on semiconducting properties are expected.

An interesting transitional behavior was observed in step-like humidity changes for sensors based on SnO_2 at considerably high temperatures (Fig. 11). This is caused by fast competitive adsorption between H_2O and adsorbed oxygen species (O^{2-}, O^-, etc.) and desorption of the adsorbed oxygen species and releasing of free electrons. This phenomenon suggests the electronic conduction mechanism and also confirms the contribution of competitive adsorption between H_2O and adsorbed oxygen to the conductivity increase. For sensors based on In_2O_3 or ZnO, similar peak patterns due to step-like humidity changes were also observed in the temperature range from 230 °C to 540 °C. The mechanism should be similar to that of SnO_2 sensors.[74]

For sensors based on ultra-thin SnO_2 films (60–90 nm) prepared by sol–gel process, the response time ranged

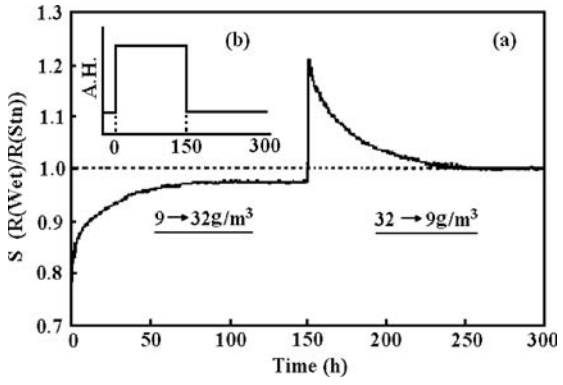

Fig. 11. (a) Typical response curves of SnO_2 under rectangular pattern of humidity change. Sensor operating temperature 460 °C, thickness 100 mm, calcination temperature 600 °C. (b) Changing humidity pattern. Reprinted with permission from [74], T. Kuse et al., *Sens. Actuators B* 67, 36 (**2000**). © 2000, Elsevier.

from 8–17 s for different humidity changes and the recovery time was only about 1 s, due to their ultra-thin films.[75] However, most reported SnO_2 sensors are only sensitive to RH higher than 30%.[75–77] In addition to sensing water vapor, SnO_2 is widely used for multiple gases, especially harmful oxides such as NO_X, CO, PbO_2. Since these sensors are usually operated at temperatures above 200 °C, heaters are always attached at the backside.[78]

3.2.2. Perovskite Compounds

The perovskite compounds belong to a large group of oxides with a general composition of AXO_3. The A can be any metal element with +2 valence electrons, e.g., group II, group IV, and rare earth metals. The X represents titanium, niobium, and iron.[79] Sometimes A or X could be a combination of two or more elements, e.g., $La_{0.7}Ca_{0.3}$ for A and $Zr_{0.2}Ti_{0.8}$ for X.[80] All members of this group have the same basic structure that is isometric.

Perovskite oxides form a group of ceramics that exhibit a variety of interesting properties and promising applications. *N*-type perovskite semiconductors exhibit electrical conductivity variation as humidity changes and have high sensitivity to water partial pressure down to 0.006 atm.[81] However, as mentioned previously, like TiO_2, the humidity-sensing property of perovskite oxides is only effective at elevated temperatures (400–700 °C). Therefore, the reported perovskite oxide humidity sensing devices, based on electron-conducting mechanism, are operated at the temperature of hundreds of Celsius.[81, 82]

At room temperature, some porous perovskite oxides still demonstrate humidity sensitivity, e.g., $BaMO_3$ (with M = Ti, Zr, Hf, or Sn).[83, 84] Because the sensing mechanism is no longer electron-conducting but ion-conducting, they are only sensitive to humidity higher than 8%–20% RH.[84–86] In these cases, the porous perovskite oxides operating at room temperature may be regarded as simple resistive/capacitive ceramics, in which the group II elements may serve as metal ions to improve the conductivity in moisture. As shown in Figure 12, most humidity sensitive perovskite oxides were fabricated by bulk-sintering of the mixture of two or more metal oxides/carbonates (e.g., sintering of $SrCO_3$ and SnO_2 to obtain $SrSnO_3$[82]).

3.2.3. In_2O_3

In industry, smooth and transparent films made of indium oxide, an *n*-type ceramic semiconductor, are used as infrared-reflectors or electrodes for liquid crystals. There are a couple of methods for fabrication of rough and porous In_2O_3 layers that are sensitive to moisture. Laser ablation was reported to be a good method to sensitize ITO to humidity by producing gaps on the substrate layer.[87, 88] The humidity-sensing is due to the porous water-adsorbing structure inside the gaps. *P*-type doping with divalent anions from the VIII group (Mn^{2+}, Ni^{2+}, etc.) may also facilitate the roughness and porosity.[89] Using thermal deposition in high vacuum was found to obtain In_2O_3 films with granular sizes ranging from 1 to 10 μm.[90]

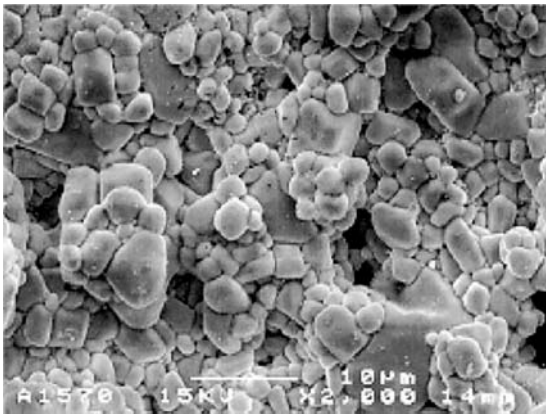

Fig. 12. $Ba_{1-x}Sr_xTiO_3$ sintered at 1050 °C. Reprinted with permission from [86], W. Qu et al., *Measurement Sci. Technol.* 11, 1111 (**2000**). © 2000, Institute of Physics.

However, none of the presented In_2O_3 humidity sensors is able to sense relative humidity lower than 25%[87–90] and the response may take a couple of minutes.[89] This type of devices still needs improvement. Although we categorize In_2O_3 as a semiconducting (electronic conducting) material, its moisture-sensing mechanism is still not very clear.

3.2.4. Other Semiconducting Sensing Materials

Homogeneously mixed and sintered ZnO–Y_2O_3 was found to be a humidity-sensitive *n*-type semiconductor.[91] Doping with Li^+ at 900 °C shows linear behavior in the entire humidity range from 5% to 98% RH at room temperatures, probably due to the larger dissociation rate of the adsorbed water molecules induced by Li^+ ions. Changing mole percentages of $ZnMoO_4$ and ZnO mixtures sintered at 900 °C was found to affect their humidity sensitivity.[92] With appropriate mole percentage, the sensor can respond to humidity as low as 5% RH.[92] The composite materials were found to be *n*-type and the electrical conduction due to the water donors was thought to be the dominant mechanism at least in the low humidity range.

3.3. Polymer-Based Humidity Sensors

Organic polymers are macromolecules in which a unit structure repeats. Most of the polymers are carbon-hydride compounds or their derivatives. The carbon atoms link each other one by one, either by sigma bond (single bond) or sigma bond plus pi bond (double bonds or triple bonds), forming a long chain, which is called the backbone of the polymer. Functional groups are rooted on the backbone, which could be either single atoms (e.g., oxygen or halogen) or molecular groups (e.g., –COOH, $–NO_2$). The functional groups, along with the basic structure of

REVIEW

the backbone, determine the chemical and physical properties of the polymers.[93] Artificial polymers are synthesized from monomers that are small molecules. Copolymers are polymers synthesized from two or more different kinds of monomers. Polymeric humidity sensors have been widely studied in research and applied in industry for more than 30 years. Most of the sensors are based on porous polymer films thinner than millimeters and their sensing principle is quite similar to that of ceramic sensors. The film is filled with micro-pores for water vapor condensation and some of the measurable physical properties change due to the water absorption.

Traditionally, according to sensing mechanisms, polymeric humidity sensors are divided into two fundamental categories: resistive-type and capacitive-type.[94] The former responds to moisture variation by changing its conductivity while the latter responds to water vapor by varying its dielectric constant. Almost all of the humidity sensors based on polymers operate at room temperature, due to polymers' high sensitivity to heat. However, during the last ten years, in addition to the traditional quaternary ammonium and sulfonate compounds,[92–96] polymers containing phosphonium have been developed for humidity sensing.[97] More importantly, copolymers and mutually reactive copolymers have also been studied for humidity sensing.[98] Humidity sensors based on conjugated polymers that are conductive polymers but not polymeric electrolytes attract considerable attention in research laboratories and industries.[99, 100] These new materials along with ammonium and sulfonate polymers will be discussed in detail in this section. In addition, polymeric humidity sensors other than electrical impedance measurements (conductance and capacitance), such as piezoresistive[101] and surface wave acoustic (SAW)[102] devices, will also be described in this section. Optical sensors, in which polymers are used to coat fibers,[103] will not be discussed in this section.

3.3.1. Polyelectrolyte-Based Resistive Sensors

Almost all of the polymeric resistive humidity sensors are based on two types of materials: polyelectrolytes and conjugated polymers. For both types of materials, the conductivity of most polymers decreases with increasing humidity level. However, the conductivity of the former is always lower, due to its ionic functional groups. Generally speaking, polyelectrolytes are hydrophilic or even water-soluble, while conjugated polymers (conducting or semiconducting polymers) are rather hydrophobic and unable to absorb much water. To fabricate humidity sensors based on polyelectrolytes, it is reasonable to use some methods to avoid deformation caused by dissolving[94] and to enhance the sensitivity by lowering the intrinsic conductivity.[104] For sensors based on conducting/semiconducting polymers, dispersing some ions inside the materials leads to reduction in resistivity at low RH[99] and thus generates greater absolute signals. The configuration of most resistive sensors, as well as of capacitive sensors that will be discussed later, is either a sandwiched structure with electrodes on both sides or interdigited electrodes with deposited polymer films in between. For the sandwiched structure, the top electrode is always a vapor-permeable thin metal film, e.g., gold.

Polyelectrolytes are polymers with electrolytic groups, which could be salts, acids, and bases. Based on functional groups, humidity-sensitive polyelectrolytes can be fundamentally divided into three major categories: quaternary ammonium salts,[105–113] sulfonate salts,[114, 115] and phosphonium salts.[97, 98, 116–118] To absorb moisture, the polyelectrolytes are usually prepared as porous thin films. Ammonium and sulfonate salts are traditional polyelectrolytes used in moisture sensing. During the last few years, phosphonium salts were developed. Since phosphorous is just below nitrogen in the periodic table, the chemical properties of phosphonium are nearly identical to those of ammonium. Sometimes phosphonium salts are favored in humidity sensing due to the easy formation of organic quaternary phosphonium with vinyl monomers.[118] As shown in Figure 13, Cl^- is a counter ion in dimethyldiallylammonium chloride, while Na^+ is a counter ion in poly(sodium *p*-styrene sulfonate). Apparently, the mobility of the counter ions in polyelectrolytes is very high.

In addition to the ionic compounds introduced above, it is reported that KOH (potassium hydroxide)-H_2O-doped PVA (poly(vinyl alcohol)) is sensitive to RH over 50%.[119] The backbones of the polyelectrolytes are commonly hydrophobic, while the electrolytic groups are quite soluble in water. As water absorbed on these porous films, the conduction mechanism is similar to that of the zeolites doped with electrolyte ions, which is a water-phase electrolyte material (see Section 3.1). Ions dissolved in the water layer formed by absorption become carriers of electric conduction. The counter ions comprise the majority of the carriers due to their high mobility. The conductivity of the films increases as humidity increases. From their structures, it is easy to find three major drawbacks of the porous films made of polyelectrolytes. First, the materials are soluble in water and the counter ions are ready to exchange with H^+ or OH^-, especially at high humidity levels or in cases when dews form. Second, deformation due to change of humidity or temperature lowers their performance and shortens their lifetime. Additionally, due to their high solubility the conductivity reaches a very high value even if humidity is little. Therefore their sensitivity to high RH is quite weak.

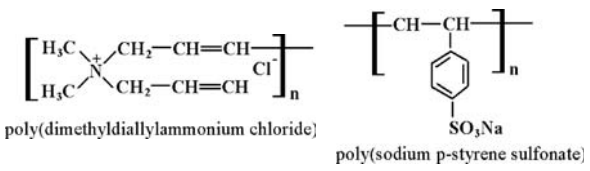

Fig. 13. Two typical polyelectrolytes.

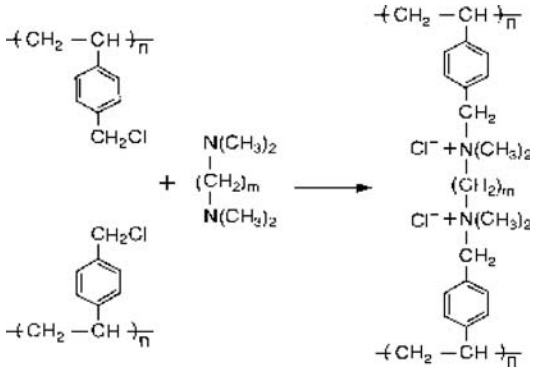

Fig. 14. Simultaneous cross-linking and quaternization of poly chloromethyl styrene with diaminoalkane. Reprinted with permission from [107], Y. Sakai et al., *Sens. Actuators B* 66, 135 **(2000)**. © 2000, Elsevier.

Back to 1839, Charles Goodyear vulcanized natural rubber using sulfur by cross-linking the isolated polymeric rubber chains into an intensive network.[120] For humidity sensing polyelectrolytic films, the same method (cross-linking) is used to enhance the mechanical properties of the sensors, as well as preventing dissolving of ions and strengthening the adherence to the substrate.[97, 98, 105–108, 112–117] Figure 14 shows a cross-linking reaction.[107] The diaminoalkane (the compound at the center) forms a "bridge" that connects two polymer chains together so that a dense, insoluble, and intensive polymer network is resulted. Note that the cross-linking reagent (diaminoalkane) becomes the electrolytic (humidity-sensitive) group of the network and the cross-linking and ammonium-quaternization are accomplished at the same time.

In many cases, simple cross-linking cannot assure satisfactory insolubility, lifetime, and intensity. Based on cross-linking interpenetrating polymer network (IPN) has been developed.[106, 115] IPN consists of a cross-linked polyelectrolyte and a cross-linked hydrophobic polymer. The two cross-linked polymers interpenetrate each other. Figure 15 shows two typical IPNs, the ethylene glycol dimethacrylate (EGDMA) that is a cross-linked hydrophobic polymer and poly(AMPS-co-PGM) that is a cross-linked polyelectrolyte. AMPS means 2-acrylamido-2-methylpropane sulfonic acid and PGM means polypropylene glycol monomethacrylate. poly(AMPS-co-PGM) is a copolymer synthesized from the mixture of AMPS and PGM monomers. Melamine resin cross-links the poly(AMPS-co-PGM) chains.

In addition to using chemical reagents, the cross-linking can also be accomplished by Co^{60} radiation as well as by the radiation of UV light.[105, 121, 122] Graft-polymerizing, in which electrolytic groups are grafted on a pre-prepared polymer backbone that comprises a porous film, is also a good method to make the sensing film resistive to water.[94] The cross-linking and IPN are primarily dealing with the solubility and deformation, but have little to do with

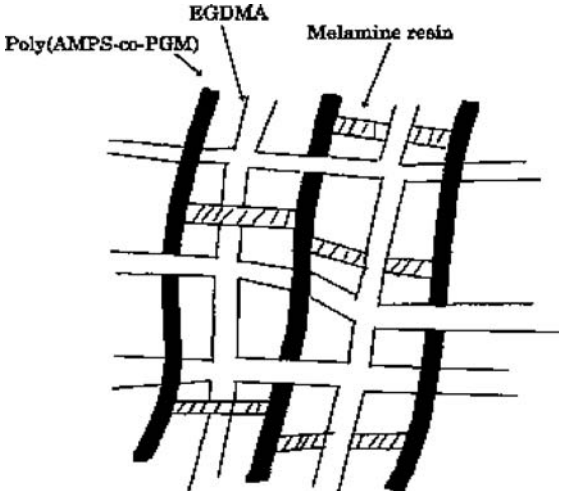

Fig. 15. Interpenetrating polymer networks (IPN). Reprinted with permission from [115], Y. Sakai et al., *Electrochim. Acta* 46, 1509 **(2001)**. © 2001, Elsevier.

enhancement of sensitivity. The sensitivity becomes quite low at high humidity due to its low resistivity at low RH. According to researchers,[97, 98, 108–118] this problem can be solved by adding some insulating content into the highly conductive polyelectrolytes. The inserted insulting parts is able to absorb enough water, dilute the ion concentration, and limit the mobility of ions.[104] Therefore, hygroscopic insulating polymers, like PVA and polyesters, are always favored. This method is proved to be effective for lowering the conductivity of polyelectrolytes at low RH and enhancing sensitivity at high RH. Figure 16 illustrates a typical

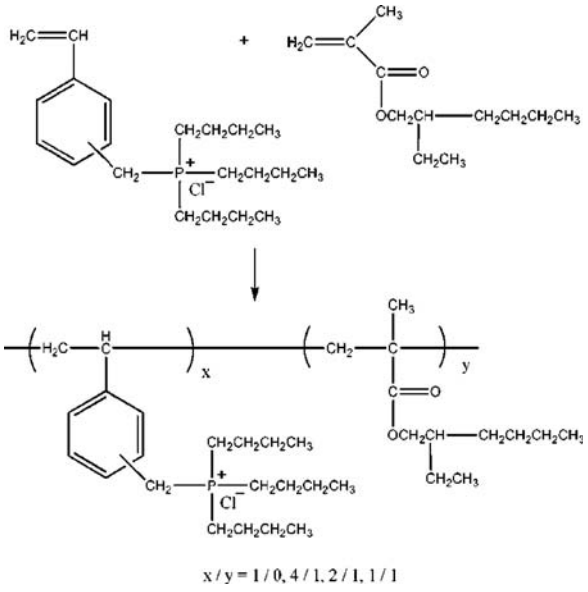

Fig. 16. Reaction to form a copolymer. Reprinted with permission from [117], M. S. Gong et al., *J. Mater. Sci.* 37, 4615 **(2002)**. © 2002, Elsevier.

REVIEW

synthesis reaction for preparing a copolymer, i.e., mixing two monomers in appropriate solvent under proper conditions. The reactant on the left is the electrolyte, (vinylbenyl) tributylphosphonium chloride, and on the right is the hygroscopic insulating compound, an ester.

Humidity-sensitive copolymer films can also be cross-linked to enhance the performance,[97, 108, 116, 118] or even form IPNs with a cross-linked hydrophobic polymer.[115] Recently, cross-linked copolymers resulted from mutually reactive polymers have been developed.[98, 110–113] Different from traditional cross-linking, in which chains of the same polymer are jointed together, two different polymers (mutually reactive polymers) are bridged together in this process. There is no bridging reagent or radiation needed in the cross-linking process and the connection between the two reagents is accomplished by direct reactions. At least one of the two mutually reactive polymers (reagents) is a copolymer as discussed in the above few paragraphs. A mutually reactive cross-linking is illustrated in Figure 17[110] and the quarternization is finished simultaneously.

The product of the reaction in Figure 17 is somewhat similar to the IPN (see Fig. 15). This indicates that the cross-linked structure from mutually reactive polymers may have mechanical properties as good as IPNs, of which the process is much more complicated. Based on polyelectrolytes, many humidity sensors are able to response to RH from 20% to 90% with good linearity[98, 108, 110–112, 116–118] and some of them are even sensitive to RH around 10%.[106, 107]

3.3.2. Conducting/Semiconducting Polymers

In polymers and single molecules, sometimes double bonds and single bond may occur alternately along the main chain. This structure is called conjugation, which is a key thing for semiconductive and conductive polymers. A conjugation structure existing along the entire main chain is named universal conjugation (Fig. 18). Conductive polymers were first reported in 1977.[123] As verified by theories and experiments,[124] the greater the degree of conjugation, the narrower is the band gap, because more bonding electrons are delocalized. The band gap of highly conjugated polymers is small (∼2 eV) and that of saturated polymers is high (∼10 eV). The reason for the decreasing band gap is that the conjugating structure delocalizes the bonding electrons and the system energy is reduced. If the conjugation is universal, its degree can be represented by the degree of polymerization. For highly conjugated polymers with high polymerization degree, the intermolecular resistance becomes negligible in the bulk. This is because the intermolecular energy gap for charge carrier to overcome is quite small, which is usually less than 0.1 eV for high degree of polymerization due to the Van der Waals force that increases with mass.

Like intrinsic silicon, despite containing universally conjugated chains the intrinsic conducting polymers are

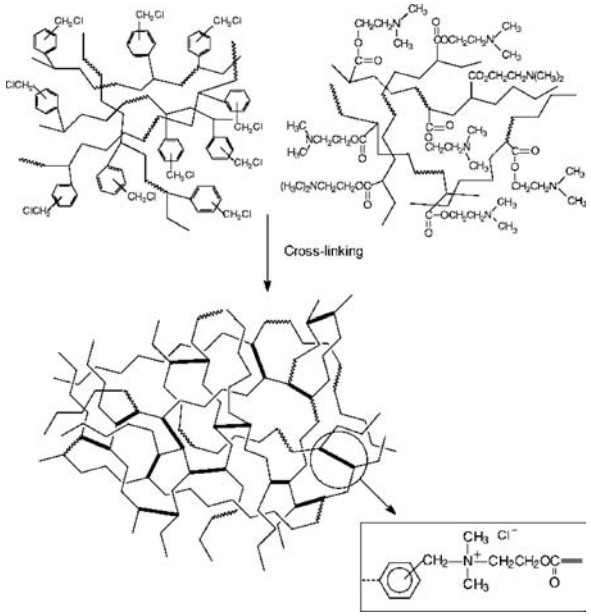

Fig. 17. Cross-linking by mutually reactive copolymers. Reprinted with permission from [110], S. H. Park et al., *Sens. Actuators B* 86, 68 (**2002**). © 2002, Elsevier.

not very conductive because of shortage of free charge carriers. Also, radiation with photon energy higher than the band gap could enhance the conductivity by exciting electrons from the valence band to the conduction band. The conducting mechanism of intrinsic polymers could be interpreted by the principles of electron–hole pair traveling under electric field.[125] However, the traveling is one-dimensional rather than three-dimensional due to the structure of conjugated polymers. Since most conductive polymers lack completely equivalent carbon sites along the main chain, some charges are localized and the band gap is therefore enlarged. The sites that trap the carriers are named polarons (a polaron with two charges is called a "bipolaron") and the process in which carriers overcome the polaron barrier(s) is called "hopping."

At room temperature, the conductivity of intrinsic polyacetylene is very low, only 10^{-7} to 10^{-8} S cm^{-1} (that of intrinsic silicon is about 4×10^{-6} S cm^{-1}). Similar to inorganic semiconductors, the conductivity of polymers can be considerably enhanced by doping. The doping of polymers is actually to oxidize (*p*-type doping) or reduce (*n*-type doping) the backbone by chemical agents.[126, 127] The oxidation/reduction also generates by-products, like positive or negative ions. These ions become part of the

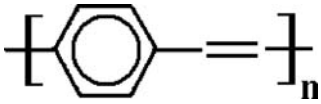

Fig. 18. Poly(*p*-phenylene vinylene), a typical conducting polymer with universal conjugation.

polymer to keep the net charge to be zero. They are usually called "counter ions." It is expected that a *p*-type polymer semiconductor may contain negative counter ions and an *n*-type one may contain positive counter ions. In case that sufficient amount of water is absorbed on the doped polymers, one may expect that polymers may show some ionic conduction with the counter ions as the carriers. It is known that the conductivity of extrinsic silicon is very high ($>1000\ S\,cm^{-1}$). However, for general polymers (polyacetylene or polyphenylene) with moderate doping (either *p*-type or *n*-type), the conductivity may vary from 0.1 to 1 $S\,cm^{-1}$. In recent years, several devices based on conducting/semiconducting polymers were built, including LEDs,[128] solar cells,[129] and field-effect transistors.[130]

Water is well known for its protonation and the released proton interacts with universally conjugated C=C double bonds. This effect was discovered and used for humidity sensing. Generally, dopants always play an important role in the conductivity variation caused by absorbed water.[131, 132] As conducting polymers, polyaniline (PANI) and its derivatives have been found to be humidity-sensitive for a long time.[133–135] Due to polymerization by some strong oxidant (e.g., $(NH_4)_2S_2O_8$), the PANI structure contains two basic forms: non-oxidized (reduced) and oxidized structures (Fig. 19). Apparently, the PANI synthesized in this way may be regarded as *p*-type doping. Due to the un-bonded electron pair on the nitrogen atom, both forms can be protonated: $—NH— \rightarrow —NH_2^+—$ and $—N= \rightarrow —NH^+=$. According to a buildup model,[133, 136] the electron transferring (hopping) from the protonated reduced form ($—NH_2^+—$) to the protonated oxidized form ($—NH^+=$) is the dominant conduction process of PANI when water content reaches 0.1% (mole ratio). Since in this process a proton is transferred to water by the reaction, $—NH_2^+— + H_2O \rightarrow —NH^+= + H_3O^+$, absorbed water plays an important role in the conductivity. The humidity-sensing property of PANI to water vapor can be regarded as electron hopping assisted by proton exchange. Its conduction is both electronic and ionic. The ionic conduction is favorable as long as mobile counter ions (for example, Cl^-) exist in the polymer.[135] Although it is verified that PANI and its derivative are sensitive to humidity, the response is very low due to weak hygroscopicity, at most one order of magnitude change in conductivity.[133, 136] Using a similar methodology in polyelectrolytes, some researchers combine (o-phenylenediamine) (PoPD, a close

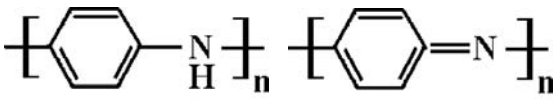

Fig. 19. Two redox forms of polyaniline (in the reduced form, the unbonded electron pair on the nitrogen atom contributes to the conjugation).

structure to PANI) with hygroscopic polymers like PVA to enhance the response.[99, 137, 138] The hygroscopic PVA absorbs water molecules from poly in the drying stage and provides water molecules to PoPD as humidity increases. As reported, the composite PoPD/PVA is able to detect RH below 10%.[99, 137] Some hysteresis is observed in this type of sensor after long-term operation or short exposure to high humidity. Researchers attribute it to a layer of sulfuric acid that is formed from the dopant (fuming sulfuric acid).[137] A major drawback of PANI is its poor processibility. It is reported that converting PANA (Poly (anthranilic acid)) into PANI by heat treatment turns to be a convenient method for fabricating PANI with good humidity-sensing property.[139] The doped composite film of poly(o-anisidine)/PVA, which is also a derivative of PANI, was reported to be humidity-sensitive.[140]

Poly(*p*-diethynylbenzene) or PDEB is a conducting polymer due to its long-chain conjugated structure. As reported in Ref. [100], PDEB synthesized by some organic nickel catalyst is sensitive to RH ranging from 10% to 90% with rather low impedance. More recently, the same research group reported other conducting polymers, such as Poly(propargyl benzoate) (PPBT),[141] *p*-diethynylbenzene-co-propargyl alcohol,[142] and ethynylbenzene-co-propargyl alcohol (copolymer),[143] are also good candidates for humidity sensing. All the above sensing polymers are synthesized using the same organic palladium as the polymerization catalyst and doped with $FeCl_3$, except for PDEB (nickel-catalyzed without Fe-doping) and PPBT (palladium-catalyzed without Fe-doping). The synthesized PPBT and PA-co-OHP bilayer also response to RH as low as 10%[141] and the other two copolymers only response to RH over 30%.[142, 143] The merit of ethynylbenzene-co-propargyl alcohol is that for RH over 30% the logarithm of the capacitance of the film changes linearly with humidity and its sensitivity is very high.[143] The sensing mechanism may be due to the interaction between protons or dopant ions and the universally conjugated structure.[100, 141, 142] For PDEB and PPBT that are not doped with $FeCl_3$, the catalyst (nickel or palladium) may play an important role in conductivity by doping ions into the polymers.

3.3.3. Hydrophobic Polymer-Based Capacitive Sensors

Unlike resistive sensors based on polyelectrolytes, capacitive polymer films for humidity-sensing are made from hydrophobic organic materials that are somewhat hygroscopic in order to absorb moisture.[94] In other words, the polymers for capacitive sensors should be both non-ionic and highly polar macromolecules. In the market, capacitive sensors are usually more expensive than resistive sensors due to their high fabrication cost.[144] However, with excellent linear response,[144–146] capacitive sensors are far more attractive than resistive sensors. This linear response is due to a very simple principle described

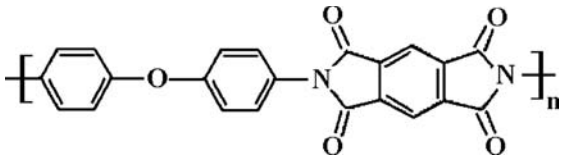

Fig. 20. Kapton, a typical polyimide.

as follows. For insulating polymers, the absorbed water, the weight of which is proportional to relative humidity, occupies the free space between the polymeric molecules. Therefore the change of the dielectric constant of the hygroscopic polymer is linearly proportional to the amount of water absorbed. To be non-ionic but very polar, polyimides,[144–149] and esters are apparently good candidates, such as cellulose acetate butyrate (CAB),[150–152] poly(methyl methacrylate) (PMMA),[153, 154] poly(vinyl crotonate),[121] and poly(ethyleneterephthalate) (PETT).[155] Figure 20 illustrates a typical polymer for capacitive humidity-sensing. Models for moisture sensing in both materials have been established.[144, 150] Hysteresis is usually a serious problem in capacitive sensors. Hysteresis comes from clusters of absorbed water inside the bulk polymer.[94, 152] Formation of clusters indicates that hygroscopicity of some polymers is too high and relatively large voids exist in the polymeric structures. The water clusters may also deform the polymers and shorten the lifetimes of the sensors.

In the previous section (Section 3.2.1), we discussed the application of cross-linking to solve the deformation and aging caused by water absorbed in polyelectrolytes. For capacitive sensors, the cross-linking method,[121, 122, 153, 154] in which hygroscopicity is lowered and the resistance is enhanced due to temperature change,[121] is also used to against the hysteresis. Some hygroscopic cross-linking agents can also enhance the sensitivity of the film.[154] Polyimides, which are used as insulators in integrated circuits,[147, 148] are the most commonly used group of materials for capacitive humidity sensors[94, 144–148] and the response is always linear with the detection limit generally below 20% RH. In addition, polyimides can also be used as substrates for humidity sensors.[149] The polyimide (Kapton) can be doped with carbon to become conductive. Between the polyimide substrate and the sensing film (made of other polymers), the adherence is strong and the mismatch in thermal coefficients is small. It is also reported that carbon filled polysulfone can be used as good electrodes for humidity sensors based on polyimides.[145]

Other polymers suitable for capacitive humidity sensors include polyethersulphone (PES),[144] polysulfone (PSF),[156] divinyl siloxane benzocyclobutene (BCB),[157] hexamethyldisilazane (HMDSN),[158] etc. The capacitive humidity sensors have linear response as low as 15% RH[121, 144, 148, 155] and some have very low hysteresis (<2%).[144, 146, 156]

4. ABSOLUTE HUMIDITY SENSORS (HYGROMETERS)

In early years, meteorologists were interested in an instrument capable of measuring the water content of the upper air latitudes where the water concentration was less than 10 ppmv at air temperature of −56 °C.[159] In 1948, a dew/frost hygrometer based on moisture condensation on a mirror was developed to measure the absolute humidity in extremely dry air of stratosphere with the lowest detectable humidity level of −90 °C frost point.[159] In 1967, a fully automated dew/frost point hygrometer based on a mirror with much better performance was developed with much faster response.[160] In 1978, a solid-state moisture sensor based on porous anodic aluminum oxide was developed with fast response and wide measurement range (−110 °C to +50 °C).[161] In following two sections, we will review the mirror-based hygrometers and solid-based moisture sensors.

4.1. Mirror-Based Dew/Frost Point Sensors (Hygrometers)

The basic structure of a dew/frost hygrometer is shown in Figure 21.[160] Light from the Farmer electric lamp is projected onto the sensing element and is received by the photo resistor. If water condenses on the gold mirror of the sensing element, the photo resistor picks up the optical signal and the corresponding temperature is recorded. During 1990s, people had renewed interests in improvement of the mirror-based dew/frost hygrometers. The improvement was focused on the sensing element, i.e., how to accurately detect temperature at which water begins to condense on the mirror surface? In order to stabilize the mirror temperature, additional heat was injected into the mirror.[162, 163] The experimental results showed that temperature was many times faster and over-condensation was minimized. The temperature fluctuations around the dew point usually were not over 0.03 K. During the hygrometer operation, the heat pump cools the mirror and simultaneously gives out a huge amount of heat into the heat housing. This temperature change influences the sensitivity of the optical dew detector, which decreases the hygrometer's accuracy. In order to solve this problem, optical fibers were used to separate the optical dew detector from the mirror area as shown in Figure 22.[164] The accuracy of the hygrometer was significantly improved at elevated temperatures. At 50 °C, the error of the fiber optical dew detector is ∼−0.10 to −0.11 °C while the regular optical dew detector is ∼−0.63 to −0.65 °C.[164] It was shown that the dew could be detected from the laser light scattered from the rough surface of a metal plate instead of the mirror surface.[165] The dew point was determined with an accuracy of ±0.5 °C, corresponding to ±2% in relative humidity at a temperature of 27 °C. The laser light was supplied through an optical fiber from a laser

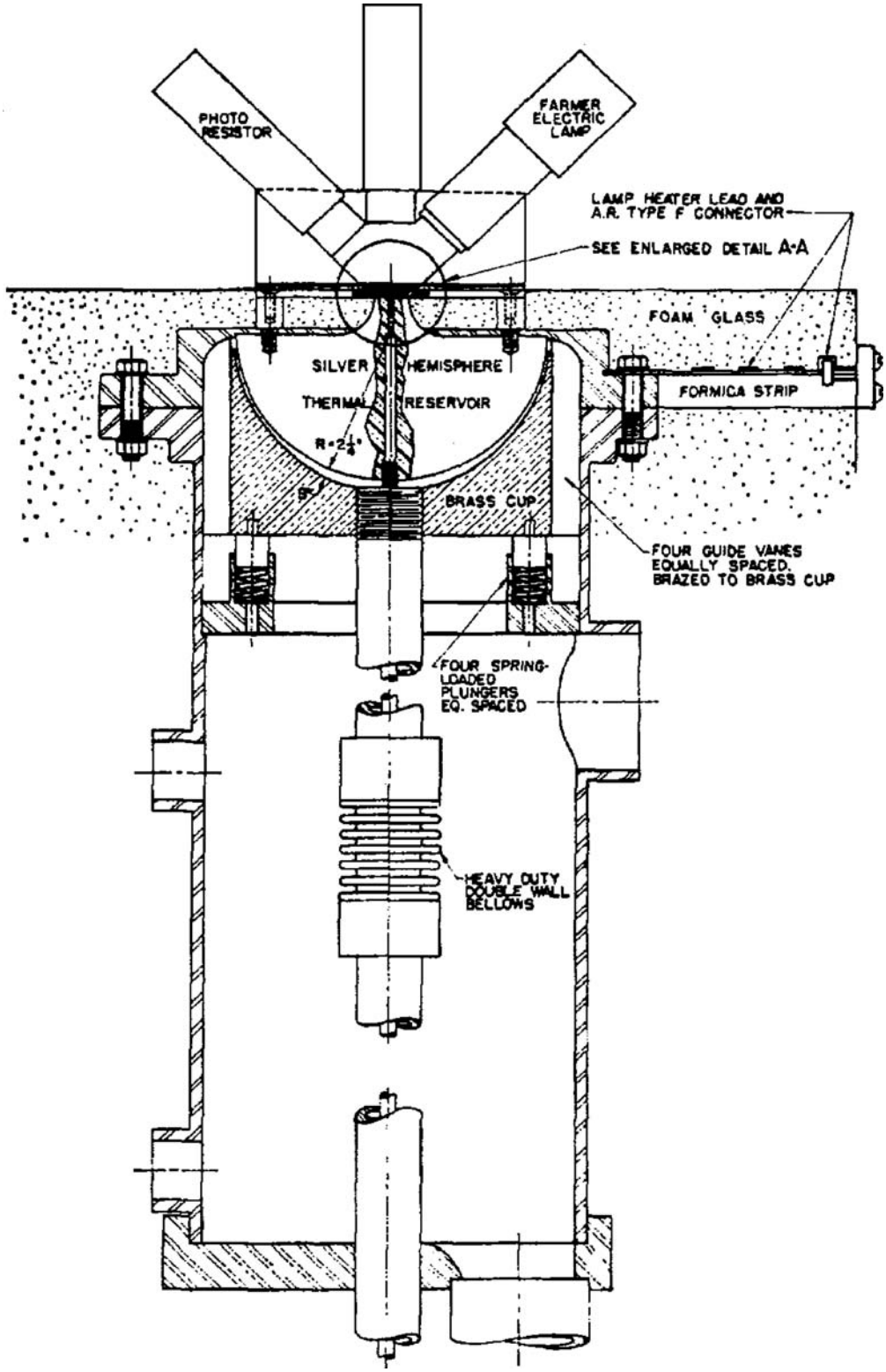

Fig. 21. Frost/dew point hygrometer assembly. Reprinted with permission from [160], S. H. Jury et al., *Anal. Chem.* 39, 912 **(1967)**. © 1967, American Chemical Society.

REVIEW

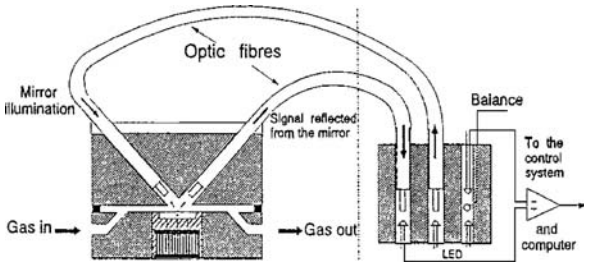

Fig. 22. Schematic of the hygrometer measurement head with fiber optical dew point detector. Reprinted with permission from [164], R. S. Jachowicz et al., *Sens. Actuators A* 42, 503 **(1994)**. © 1994, Elsevier.

diode and the scattered laser light was transmitted to a phototransistor also through an optical fiber. The response time of this laser dew-point hygrometer is ∼0.2–3 min or 12–180 s.[166] Although the absolute humidity is temperature independent, the technique for dew point measurement is still temperature dependent. One way to solve this problem is to use optical fiber as described above. Another way is to use a single micro-air-bridge heater to eliminate the influence of the ambient temperature in absolute humidity sensing by a thermal sensor.[167] In order to develop a new way to use a Peltier device (thermoelectric cooler) for fast humidity sensing, the optical signal of a photodetector was studied when water condensation appears on the cold side of the Peltier device.[168] The thermoelectric device was used at a pulsed rate. During cooling, the applied current is stopped as soon as a variation of the optical response, due to the appearance of water droplets, is observed. A reverse pulse is then applied to return quickly to the ambient temperature. The delay time of the optical detection is in the range of 0.25–12.2 s for humidity in the range of 15–70%.[168] The schematic of the optical dew detector is shown in Figure 23.[169] It is composed of a single-stage thermoelectric cooler stuck

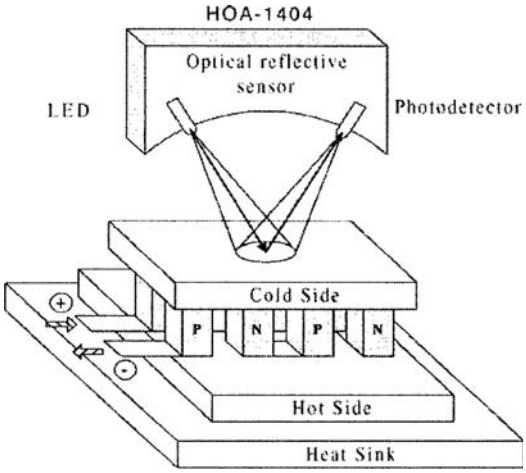

Fig. 23. Schematic of the dew point sensor. Reprinted with permission from [169], B. Sorli et al., *Sens. Actuators A* 100, 24 **(2002)**. © 2002, Elsevier.

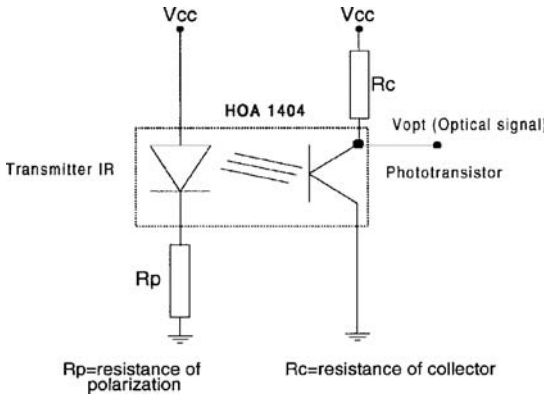

Fig. 24. Optocoupler polarization. Reprinted with permission from [169], B. Sorli et al., *Sens. Actuators A* 100, 24 **(2002)**. © 2002, Elsevier.

on a copper sink. A commercial optocoupler (Honeywell HOA-1404) is placed in front of the cold side of the thermoelectric cooler (Peltier device). The optimal photo signal is obtained as a function of the focal length. The signal coming from the detector is a function of the optical reflection. The phototransistor of the optocoupler is polarized according to Figure 24 so that the optical signal (V_{opt}) correlates with the collector-emitter voltage (V_{ce}) of the phototransistor. When water condenses on the cold side of the Peltier device, the IR light reflection is reduced, leading to lower collector current, and consequently V_{ce} increases.

Despite of their wide use, optical dew point hygrometers have several drawbacks including high cost, frequent mirror contamination, and instability under continuous use. Dew point hygrometers based on direct mass measurements of condensation have the potential to provide more accurate dew point measurement with high resolution. Surface acoustic wave (SAW) devices have been used as highly sensitive gas sensors.[170–173] It was suggested that a SAW sensor can measure mass with sensitivity 200 times greater than bulk wave sensors (quartz microbalance) due to its higher operating frequency. A review paper on gravimetric sensors for chemical applications by Ward and Buttry in 1990[174] listed a minimum mass sensitivity of 1.2 ng cm^{-2} for SAW sensors compared to 10 ng cm^{-2} for a quartz microbalance. A dew point hygrometer using a SAW sensor was developed in 1983 by Kuisma and Wiik.[175] They used SAW attenuation to detect condensation and measured temperature with an RTD. This instrument offered no apparent advantages over optical dew point hygrometers in resolution, accuracy, and cost. In 1995, Galipeau et al.[176] demonstrated an SAW dew point hygrometer with ability to accurately measure condensation surface density and dew point using SAW velocity. A condensation surface density of 3.0 ng cm^{-2} was detected. In the same year, Hoummady et al.[177] developed a dew point detector using an LST-cut quartz SAW sensor.

SAW devices increase considerably the accuracy of humidity measurement because of their dual ability to

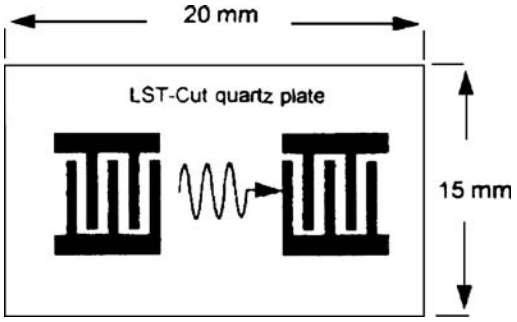

Fig. 25. The experimental surface acoustic wave delay line configuration. Reprinted with permission from [177], M. Hoummady et al., *Sens. Actuators B* 27, 315 **(1995)**. © 1995, Elsevier.

detect dew condensation and to measure the temperature with a great accuracy. The experimental SAW device is cooled using a Peltier device. When water vapor condensation appears on the Rayleigh wave propagation path, it induces a substantial attenuation of the wave amplitude and a shift in the associate oscillator's frequency (mass loading). Figure 25 shows a schematic of a SAW device based on a quartz substrate.[177] The quartz cut was an LST-cut because of its high thermal sensitivity and good linearity. The interdigital transducers are photolithographically patterned on an aluminum film of 1500 Å. The wavelength was 34.4 μm and the operating frequency about 98 MHz. The SAW device was placed in an oscillator loop. The quartz plate was cooled by means of a Peltier device glued on the bottom face (Fig. 26) in order to condense the water vapor on the SAW propagation path. The hot side of the Peltier element was water cooled. It has been shown that the amplitude depends minimally on the temperature while decreases rapidly when sufficient water vapor condenses on the quartz plate. This effect depends on the dew thickness/acoustic wavelength ratio. The frequency measurement was used for detecting dew deposition.[177] In comparison with the optical dew point detectors, the accuracy of the SAW devices was improved by about a factor of 500.[177] Coating of the SAW device with Teflon AF reduces contamination build-up and allows for accurate

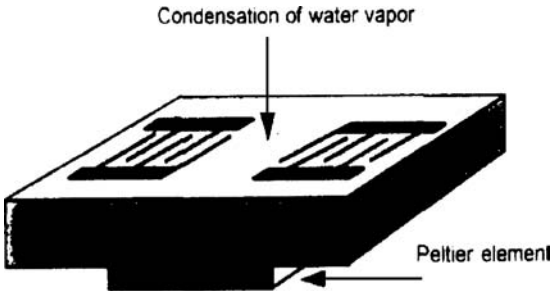

Fig. 26. Principle of an acoustic wave dew point sensor. Reprinted with permission from [177], M. Hoummady et al., *Sens. Actuators B* 27, 315 **(1995)**. © 1995, Elsevier.

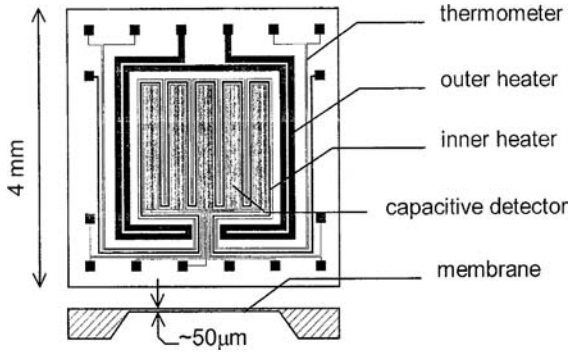

Fig. 27. The silicon dew point sensor. Reprinted with permission from [179], R. Jachowicz and J. Weremczuk, *Sens. Actuators A* 85, 75 **(2000)**. © 2000, Elsevier.

dew point measurement with improved response time at very low water vapor concentration.[178]

Water molecules exist in the form of either ice crystals or liquid water (called sub-cooled water) at negative temperatures. Generally, in nature, sub-cooled water is not stable and spontaneously converts into ice. However, on the mirror of a dew point hygrometer, this phenomenon may persist for hours. The partial pressure of saturated water vapor over a mirror is different for a mirror covered by ice than for a mirror covered by sub-cooled water even at the same temperature.[179] Therefore, in the temperature range of potential sub-cooled water presence (from 0 °C to −40 °C), the hygrometer can measure either frost point or dew point, where there is a temperature difference ΔT. The sub-cooled water error ΔT is about −1 °C per each 10 °C below zero. In order to solve the sub-cooled water issue, a silicon dew point detector was designed as shown in Figure 27.[179,180] The dew point temperature was measured with an embedded RTD thermometer. The capacitive detector was used for water and ice recognition. Two heaters were also designed with one located in the membrane (inner heater) and the other in the solid structure (outer heater) for fast temperature control surrounded both the detector and the thermometer. A model was developed to describe the water vapor contained in the measured gas, water mass transport, heat transport across the measurement head, silicon dew detector, and regulator characteristics.[181]

4.2. Aluminum Oxide Moisture Sensors

In the above section, the moisture level is measured by detecting the dew/frost point when the mirror is cooled to a point where water vapor condenses on it. The dew/frost point hygrometer is a complex system, which usually has very high cost. It will be very useful if a solid state sensor can be developed for absolute humidity measurement. Most humidity sensors were found applications in the relative humidity (RH) range. Only aluminum

REVIEW

Table I. Device failure and water vapor concentration.[161]

Failure modes	Water vapor concentration (ppmv)	
	Demonstrated failures	Failure-free upper limits
Nichrome disappearance	5,000 to 10,000	500
Aluminum disappearance	50,000 to 250,000	1,000
Gold migration	15,000 to 150,000	1,000
MOS inversion	5,000 to 20,000	200

oxide thin film sensor can be used for absolute humidity measurement.[161, 182–184]

Failure analysis of integrated circuit packages identified moisture trapped within the hermetically sealed enclosure as a major reliability problem throughout the semiconductor industry. Table I shows the failure-free upper limit of moisture level for device reliability. Water vapor can cause nichrome disappearance, gold migration, and MOS inversion. In the second column, the water vapor concentration was listed where these failures were demonstrated. The last column lists the failure-free upper limit. The failure-free upper limits are less than 1,000 ppmv. Kovac et al.[161, 182] developed an aluminum oxide sensor for *in-situ* monitoring of sealed integrated circuit packages. The sensor can respond to a moisture level as low as 1 ppmv (−76 °C dew/frost point). It is basically a capacitor-like structure consisting of a bottom aluminum electrode, an anodized porous Al_2O_3 film, and a thin, water permeable gold top electrode (Fig. 28).[161] Based on an equivalent circuit model,[161] the porous Al_2O_3 film capacitive sensor is represented by parallel resistance and capacitance. When water vapor is transported through the permeable gold layer and equilibrates on the pore walls, the number of water molecules absorbed on the pore determines the total complex impedence of the sensor. Using an admittance amplifier, a characteristic curve such as that shown in Figure 29 is obtained for the device. The "meter reading" is proportional to the admittance of the sensor. As the moisture level decreases, the admittance decreases. At a given pressure, there is a one to one correspondence between the dew/frost point and the parts per million of water vapor.

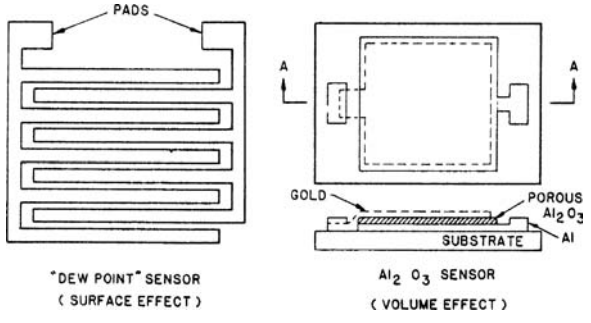

Fig. 28. Two types of moisture sensors. Reprinted with permission from [161], M. G. Kovac et al., *Solid State Technol.* 21, 35 **(1978)**. © 1978, PennWell Corporation.

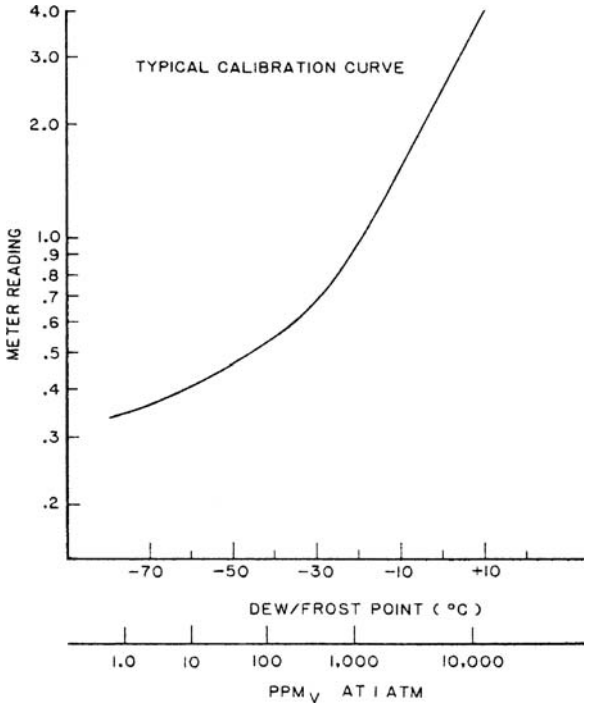

Fig. 29. Typical calibration of an industrial type Al_2O_3 moisture sensor. Reprinted with permission from [161], M. G. Kovac et al., *Solid State Technol.* 21, 35 **(1978)**. © 1978, PennWell Corporation.

Based on the porous structure, Nahar et al.[183] proposed an improved equivalent electric circuit model. Based on their suggestion, a schematic of the circuit is shown in Figure 30. In the diagram, C_s and R_s represent the capacitance and resistance of the solid walls; C_a and R_a are the capacitance and resistance of the pore area filled with air; C_b and R_b are the capacitance and resistance of the barrier layer below the air portion. C_{eff} denotes the capacitance of the multiple-dielectric capacitor comprising the sublayers: barrier layer, chemisorbed layer, and water condensed in the pore as given by the Maxwell-Wagner effect. R_{eff} is the parallel resistance of the capacitor. Based on the equivalent circuit, the capacitance and resistance can be obtained as[183]

$$C = C_s + \frac{C_a C_b}{C_a + C_b} + C_{\text{eff}} \tag{1}$$

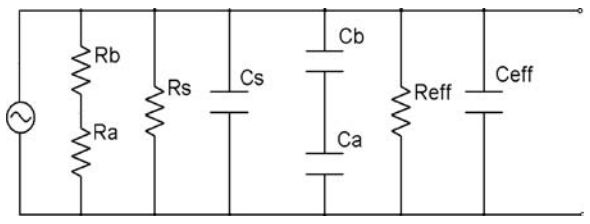

Fig. 30. Schematic of the electrical equivalent circuit model of an Al_2O_3 moisture sensor.

and

$$\frac{1}{R} = \frac{1}{R_s} + \frac{1}{R_a + R_b} + \frac{1}{R_{\text{eff}}} \quad (2)$$

On considering the actual porous structure of the anodic Al_2O_3, we have the capacitance and resistance at any humidity level[183]

$$C = \frac{\varepsilon_0 \varepsilon_s (1-\alpha) A}{d} + \varepsilon_0 \alpha A \left(\frac{x\varepsilon'}{d} + \frac{(1-x)\varepsilon_a \varepsilon_b}{\varepsilon_a b + \varepsilon_s \ell} \right) \quad (3)$$

$$R = \frac{d}{\omega \varepsilon_0 \varepsilon'' x \alpha A} \quad (4)$$

where ε_0 is the permittivity of free space, ε_s the dielectric constant of solid Al_2O_3 (value 8), ε_a dielectric constant of air (value 1), A the area of the device, α the film porosity, d the Al_2O_3 film thickness, b the barrier layer thickness, ℓ the length of the pore in which water can condense. It is a characteristic length of the sensor. x is the fraction of pore area αA filled with water. ε' and ε'' are the components of dielectric constant ε of the barrier layer-chemisorbed layer-water structure. Using this model, theoretical capacitance and resistance data were calculated.[183] The theoretical capacitance data are in good agreement with the experimental data. There is a slight deviation between the theoretical resistance data and the experimental data. Later, Nahar et al.[8, 184, 185] proposed an improved theory based on physical absorption, surface conduction mechanisms, and the dielectric properties of the Al_2O_3 film. The theoretical results are in excellent agreement with the experimental data.

There is a major drawback for aluminum oxide sensor, i.e., long-term calibration drift.[13, 186–188] The basic reason for long-term drift of sensors using porous anodic aluminum oxide films is described as follows. The structure of anodic aluminum oxide is amorphous- or γ-Al_2O_3 with hexagonal cylindrical pore structure. When the structure exposes to a humid atmosphere, the γ-phase or amorphous Al_2O_3 changes to γ-$Al_2O_3 \cdot H_2O$ (boehmite).[12] This irreversible phase change causes volume expansion of aluminum oxide, resulting in the gradual decrease of surface area and porosity.[13, 24, 25, 189] Many researchers tried to improve the anodic aluminum oxide sensors by aging the aluminum oxide in boiling water or macerating the films in some ion solutions.[13, 28, 188] However, the drift can not be completely eliminated. Even the commercial aluminum oxide moisture sensors have to be calibrated twice a year to assure their accuracy.[190] This problem seriously hinders the widespread use of aluminum oxide moisture sensors.

As mentioned in Section 3.1.1, α-Al_2O_3 is a very stable phase. However, it is very difficult to form α-Al_2O_3. It is very difficult to obtain α-Al_2O_3, because the temperature for phase change from γ to α is at least 900 °C.[191] Fortunately, there is an electrochemical approach to deposit α-Al_2O_3 without high temperature process. Anodic spark deposition is a unique process for forming certain ceramic coatings. Various coatings can be formed on a wide

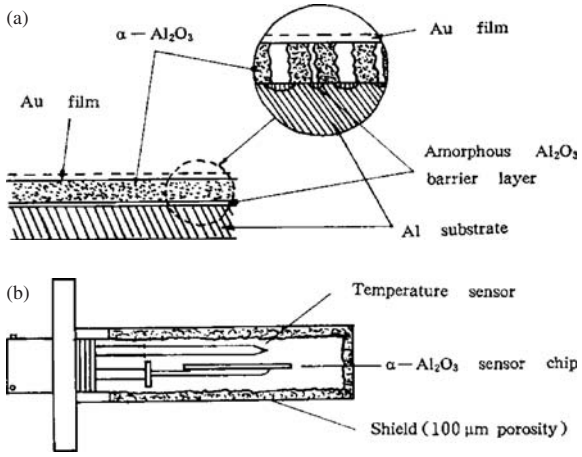

Fig. 31. (a) Schematic structure of the α-Al_2O_3 moisture sensor chip (the detailed structure is shown in the inset); (b) The moisture sensing probe assembly. Reprinted with permission from [25], Z. Chen et al., in *Proc. 27th Annual Conf. IEEE Industry Appl. Soc.*, Houston, TX **(1992)**, Vol. 2, p. 1668. © 1992, IEEE.

variety of substrates by this method.[192–196] Brown et al.[194] deposited α-Al_2O_3 coatings with thickness of more than 100 μm by anodic spark deposition in aluminate aqueous solutions with 150 V applied to the anode. Because of very little porosity and large thickness, these coatings are not good candidates for humidity sensors. Tajima et al.[22] deposited porous α-Al_2O_3 films on aluminum plates with thickness less than 10 μm in a melt of bisulfates by

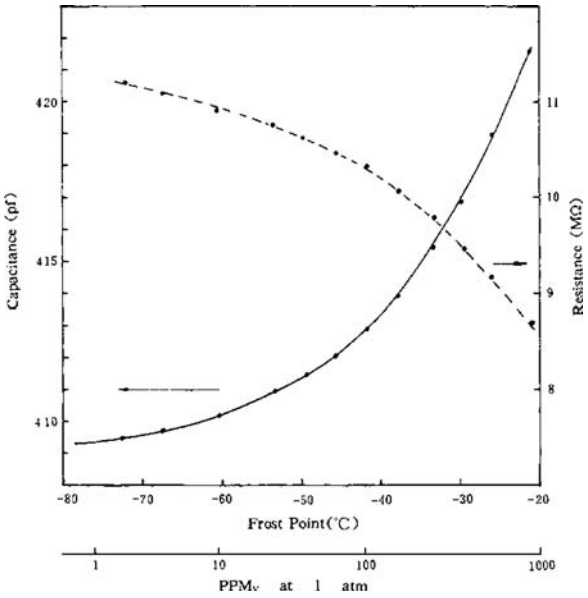

Fig. 32. Dependence of capacitance and resistance of the α-Al_2O_3 moisture sensor on absolute humidity in the trace moisture range at 0.5 V, 1 KHz, and 25 °C. Reprinted with permission from [25], Z. Chen et al., in *Proc. 27th Annual Conf. IEEE Industry Appl. Soc.*, Houston, TX **(1992)**, Vol. 2, p. 1668. © 1992, IEEE.

REVIEW

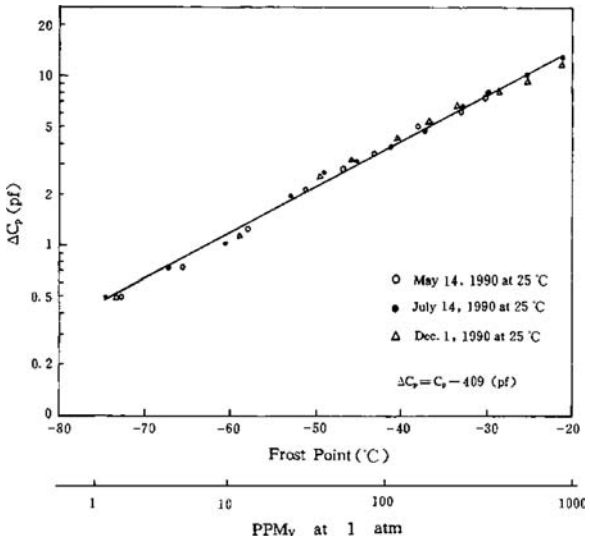

Fig. 33. Long-term stability testing results of the α-Al_2O_3 moisture sensor in the trace moisture range. Reprinted with permission from [25], Z. Chen et al., in *Proc. 27th Annual Conf. IEEE Industry Appl. Soc.*, Houston, TX **(1992)**, Vol. 2, p. 1668. © 1992, IEEE.

applying 150 V to the anode. Chen et al.[24, 25] successfully fabricated moisture sensors with capability of detecting moisture level as low as 1 ppmv using α-Al_2O_3 films formed by anodic spark deposition in the melt of $NaHSO_4$-$KHSO_4$ mixture. X-ray diffraction analysis of the sample shows a range of α phases, α(113), α(030), α(012), α(110) α(116) α(104) α(024) α(124) [a16]. Figure 6 shows the SEM images of the anodic-spark-deposited α-Al_2O_3 films.[24, 25] The average pore size is in the range from 1 to 2 μm and the porosity is about 30%. The anodic-spark-deposited α-Al_2O_3 films exhibit a continuous open pore structure, i.e., the base of the pores was the aluminum substrate, not a barrier film. This causes short circuit of the sensors when a 0.5 V (AC) voltage is applied to sensors.

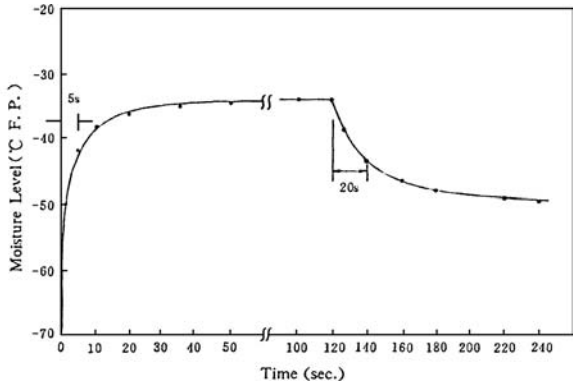

Fig. 34. Time response of the α-Al_2O_3 moisture sensor in the trace moisture range. Reprinted with permission from [25], Z. Chen et al., in *Proc. 27th Annual Conf. IEEE Industry Appl. Soc.*, Houston, TX **(1992)**, Vol. 2, p. 1668. © 1992, IEEE.

In order to overcome this difficulty, the α-Al_2O_3 film is reanodized in diluted sulfuric acid or borax solution for a short time to form a thin barrier layer as shown in the inset in Figure 31a. The schematic of the sensor structure and the moisture sensing probe is shown in Figure 31b. The fabricated sensors showed high sensitivity for moisture level from 1000 to 1 ppmv or −20 to −76 °C dew/frost point (D/F PT) (Fig. 32). The sensors also demonstrated excellent long-term stability as shown in Figure 33. For more than six months, there was no drift for data. The response was also very fast. From the low to the high moisture level the response time is about 5 s and from the high to the low moisture level about 20 s (Fig. 34). Therefore, the long-term calibration-drift occurring in γ-Al_2O_3 film sensors was eliminated in the α-Al_2O_3 film sensors.[25]

5. CONCLUSIONS

Humidity sensors based on various materials for both relative and absolute humidity have been reviewed extensively, including ceramic, semiconducting, and polymer materials. In the majority of publications, there are few papers dealing with absolute humidity sensors, which have extensive applications in industry. We reviewed extensively absolute humidity sensors in this chapter, which is unique comparing with other reviews of humidity sensors. The electrical properties of humidity sensors such as sensitivity, response time, and stability have been described in details for various materials and a considerable part of the review is focused on the sensing mechanisms. In addition, preparation and characterization of sensing materials are also described. For absolute humidity sensors, mirror-based dew point sensors and solid-state Al_2O_3 moisture sensors have been described. Each has its own advantages. Mirror-based dew-point sensors are more costly in fabrication with better accuracy, while the Al_2O_3 moisture sensors can be fabricated with low cost and used for moisture control more conveniently. As the major problem in Al_2O_3 moisture sensors, long-term instability, has been solved, α-Al_2O_3 moisture sensors may have promising future in industry.

Acknowledgments: This work is supported by National Science Foundation (EPSCoR 0447479), Department of Energy (DE-FG02-00ER4582 and DE-FG26-04NT42171), and Army Research Laboratory (W911NF-04-2-0023).

References and Notes

1. E. Traversa, *Sens. Actuators B* 23, 135 **(1995)**.
2. http://www.iceweb.com.au/Analyzer/humidity_sensors.html **(2005)**.
3. F. Ansbacher and A. C. Jason, *Nature* 24, 177 **(1953)**.
4. J. M. Thorp, *Trans. Faraday Soc.* 55, 442 **(1959)**.
5. C. J. T. de Grotthuss, Sur la Décomposition de l'eau et des Corps Qu'elle Tient en Dissolution à l'aide de l'électricité, *Galvanique. Ann. Chim.* LVIII, 54 **(1806)**.

6. T. Moromoto, M. Nagao, and F. Tokuda, *J. Phys. Chem.* 73, 243 (**1969**).
7. E. McCafferty and A. C. Zettlemoyer, *Faraday Discussions* 52, 239 (**1971**).
8. V. K. Khanna and R. K. Nahar, *J. Phys. D: Appl. Phys.* 19, L141 (**1986**).
9. Y. Yeh, T. Tseng, and D. Chang, *J. Am. Ceram. Soc.* 72, 1472 (**1989**).
10. S. Chakraborty, K. Nemoto, K. Hara, and P. T. Lai, *Smart Mater. Structure* 8, 274 (**1999**).
11. S. Chakraborty, K. Hara, and P. T. Lai, *Rev. Sci. Instrum.* 70, 1565 (**1999**).
12. L. Young, Anodic Oxide Films, Academic Press, New York (**1961**).
13. I. Emmer, Z. Hajek, and P. Repa, *Surf. Sci.* 162, 303 (**1985**).
14. R. K. Nahar and V. K. Khanna, *Sens. Actuators B* 46, 35 (**1998**).
15. E. C. Dickey, O. K. Varghese, K. G. Ong, D. Gong, M. Paulose, and C. A. Grimes, *Sensors* 2, 91 (**2002**).
16. R. K. Naharr, *Sens. Actuators B* 63, 49 (**2000**).
17. L. H. Mai, P. M. Hoa, N. T. Binh, N. Ha, and D. K. An, *Sens. Actuators B* 66, 63 (**2000**).
18. G. E. Thompson, R. C. Furneaux, G. C. Wood, J. A. Richardson, and J. S. Goode, *Nature* 272, 433 (**1978**).
19. H. Masuda and K. Fukuda, *Science* 268, 1466 (**1995**).
20. O. K. Varghese and C. A. Grimes, *J. Nanosci. Nanotechnol.* 3, 277 (**2003**).
21. S. Chakraborty, K. Nemoto, K. Hara, and P. T. Lai, *Smart Mater. Structure* 8, 274 (**1999**).
22. S. Tajima, M. Soda, T. Mori, and N. Baba, *Electrochim. Acta* 1, 205 (**1959**).
23. T. B. Van, S. D. Brown, and G. P. Wirtz, *Am. Ceram. Bull.* 56, 563 (**1977**).
24. Z. Chen, M.-C. Jin, C. Zhen, and G. Chen, *J. Am. Ceram. Soc.* 74, 1325 (**1991**).
25. Z. Chen and M.-C. Jin, in *Proc. 27th Annual Conf. IEEE Industry Appl. Soc.*, Houston, TX (**1992**), Vol. 2, p. 1668.
26. P. J. Mitchell, R. J. Mortimer, and A. Wallace, *J. Chem. Soc. Faraday Trans.* 94, 2423 (**1998**).
27. Z. Chen and M.-C. Jin, *J. Mater. Sci. Lett.* 11, 1023 (**1992**).
28. Z. Chen, M.-C. Jin, and C. Zhen, *Sens. Actuators B* 2, 167 (**1990**).
29. K. S. Shamala, L. C. S. Murthy, and K. N. Rao, *Mater. Sci. Eng. B* 106, 269 (**2004**).
30. S. Chatterjee, S. Basu, D. Chattopadhyay, K. Mistry, and K. Sengupta, *Rev. Sci. Instrum.* 72, 2792 (**2001**).
31. S. Basu, S. Chatterjee, M. Saha, S. Bandyopadhay, K. Mistry, and K. Sengupta, *Sens. Actuators B* 79, 182 (**2001**).
32. S. I. Shah, C. P. Huang, J. G. Chen, D. Doren, and M. Barteau, in Semiconductor metal oxide nanoparticles for visible light photocatalysis. *NSF Nanoscale Science and Engineering Grantees Conference*, Arlington, VA (**2003**).
33. N. Savage, B. Chwieroth, A. Ginwalla, B. R. Patton, S. A. Akbar, and P. K. Dutta, *Sens. Actuators B* 79, 17 (**2001**).
34. T. Nitta, Z. Terada, and S. Hayakawa, *J. Am. Ceram. Soc.* 63, 295 (**1980**).
35. J. Yu, X. Zhao, Q. Zhao, and G. Wang, *Mater. Chem. Phys.* 68, 253 (**2001**).
36. L. L. Chow, M. M. F. Yuen, P. C. H. Chan, and A. T. Cheung, *Sens. Actuators B* 76, 310 (**2001**).
37. B. C. Yadav and P. K. Shukla, *Ind. J. Pure Appl. Phys.* 41, 681 (**2003**).
38. X. Liu, J. Yin, Z. G. Liu, X. B. Yin, G. X. Chen, and M. Wang, *Appl. Surf. Sci.* 174, 35 (**2001**).
39. C. K. Ong and S. J. Wang, *Appl. Surf. Sci.* 185, 47 (**2001**).
40. J. Ying, C. Wan, and P. He, *Sens. Actuators B* 62, 165 (**2000**).
41. J. Slunecko, J. Holc, M. Kosec, and D. Kolar, *Informacije Midem-J. Microelectronics Electron. Comp. Mater.* 26, 285 (**1996**).
42. M. K. Jain, M. C. Bhatnagar, and G. L. Sharma, *Sens. Actuators B* 55, 180 (**1999**).
43. W. Tai and J. Oh, *Sens. Actuators B* 85, 154 (**2002**).
44. W. Tai and J. Oh, *Thin Solid Films* 422, 220 (**2002**).
45. W. Tai, J. Kim, and J. Oh, *Sens. Actuators B* 96, 477 (**2003**).
46. R. S. Niranjan, S. D. Sathaye, and I. S. Mulla, *Sens. Actuators B* 81, 64 (**2001**).
47. K. Makita, M. Nogami, and Y. Abe, *J. Mater. Sci. Lett.* 16, 550 (**1997**).
48. E. Traversa, G. Gnappi, A. Montenero, and G. Gusmano, *Sens. Actuators B* 31, 59 (**1996**).
49. R. Wu, Y. Sun, and H. Chen, *Chem. Sens.* (Suppl. B), 20, 372 (**2004**).
50. C. A. Grimes, D. Kouzoudis, E. Dickey, D. Qian, M. A. Anderson, R. Shahidain, M. Lindsey, and L. Green, *J. Appl. Phys.* 87, 5341 (**2000**).
51. S. A. Krutovertsev, A. E. Tarasova, L. S. Krutovertseva, and A. V. Zorin, *Sens. Actuators A* 62, 582 (**1997**).
52. J. Lin, M. Heurich, and E. Obermeier, *Sens. Actuators B* 13, 104 (**1993**).
53. M. d'Apuzzo, A. Aronne, S. Esposito, and P. Pernice, *J. Sol–Gel Sci. Technol.* 17, 247 (**2000**).
54. L. B. Kong, L. Y. Zhang, and X. Yao, *J. Mater. Sci. Lett.* 16, 824 (**1997**).
55. K. Robbie and M. J. Brett, *J. Vac. Sci. Technol. A* 15, 1460 (**1997**).
56. A. T. Wu1 and M. J. Brett, *Sens. Mater.* 13, 399 (**2001**).
57. K. D. Harris, A. Huizinga, and M. J. Brett, *Electrochem. Solid-State Lett.* H275 (**2002**).
58. T. Nitta, Z. Terada, and S. Hayakawa, *J. Am. Ceram. Soc.* 63, 295 (**1980**).
59. K. Arshaka, K. Twomey, and D. Egan, *Sensors* 2, 50 (**2002**).
60. M. Wu, H. Sun, and P. Li, *Sens. Actuators B* 17, 109 (**1994**).
61. G. Gusmano, G. Montesperelli, and E. Traversa, *Sens. Actuators B* 7, 460 (**1992**).
62. W. Qu and J. U. Meyer, *Measurement Sci. Technol.* 8, 593 (**1997**).
63. W. Qu and J. U. Meyer, *Sens. Actuators B* 40, 175 (**1997**).
64. U. Dellwo, P. Keller, and J. U. Meyer, *Sens. Actuators A* 61, 298 (**1997**).
65. W. Qu, W. Wlodarski, and J. U. Meyer, *Sens. Actuators B* 64, 76 (**2000**).
66. I. S. Mulla, V. A. Chaundhary, and K. Vijayamohanan, *Sens. Actuators A* 69, 72 (**1998**).
67. C. Cantalini, M. Faccio, G. Ferri, and M. Pelino, *Sens. Actuators B* 16, 293 (**1993**).
68. J. F. Boyle and K. A. Jones, *J. Electronic Mater.* 6, 717 (**1977**).
69. G. N. Avani and L. Nanis, *Sens. Actuators B* 2, 201 (**1981**).
70. N. Yamazoe, J. Fuchigami, M. Kishikawa, and T. Seiyama, *Surf. Sci.* 86, 335 (**1979**).
71. Y. Shimizu, M. Shimabukuro, H. Arai, and T. Seiyama, *J. Electrochem. Soc.* 136, 1206 (**1989**).
72. S. Mukode and H. Futata, *Sens. Actuators* 16, 1 (**1989**).
73. G. Korotchenkov, V. Brynzari, and S. Dmitriev, *Sens. Actuators B* 54, 197 (**1999**).
74. T. Kuse and S. Takahashi, *Sens. Actuators B* 67, 36 (**2000**).
75. T. M. Racheva and G. W. Critchlow, *Thin Solid Films* 292, 299 (**1997**).
76. S. G. Ansari, Z. A. Ansari, M. R. Kadam, R. N. Karekar, and R. C. Aiyer, *Sens. Actuators B* 21, 159 (**1994**).
77. L. I. Popova, S. K. Andreev, V. K. Gueorguiev, and N. D. Stoyanov, *Sens. Actuators B* 37, 1 (**1996**).
78. W. Gopel and K. D. Schierbaum, *Sens. Actuators B* 26, 1 (**1995**).
79. J. Wang, H. Wan, and Q. Lin, *Measurement Sci. Technol.* 14, 172 (**2003**).
80. S. Mathews, R. Ramesh, T. Venkatesan, and J. Benedetto, *Science* 276, 238 (**1997**).
81. W. Wang and A. V. Virkar, *Sens. Actuators B* 98, 282 (**2004**).
82. Y. Shimizu, M. Shimabukuro, H. Arai, and T. Seiyama, *J. Electrochem. Soc.* 136, 1206 (**1989**).

REVIEW

83. J. P. Lucaszewicz, *Sens. Actuators B* 4, 227 (**1991**).
84. M. Viviani, M. T. Buscaglia, V. Buscaglia, M. Leoni, and P. Nanni, *J. Euro. Ceram. Soc.* 21, 1981 (**2001**).
85. J. Holc, M. Hrovat, and J. Slunecko, *Sens. Actuators B* 26, 99 (**1995**).
86. W. Qu, R. Green, and M Austin, *Measurement Sci. Technol.* 11, 1111 (**2000**).
87. J. Kleperis, M. Kundzins, G. Vitins, V. Eglitis, G. Vaivars, and A. Lusis, *Sens. Actuators B* 28, 135 (**1995**).
88. G. Vaivars, J. Kleperis, J. Zubkans, G. Vitins, G. Liberts, and A. Lusis, *Sens. Actuators B* 33, 173 (**1996**).
89. R. B. H. Tahar, T. Ban, Y. Ohya, and Y. Takahashi, *J. Am. Ceram. Soc.* 81, 321 (**1998**).
90. K. Arshak and K. Twomey, *Sensors* 2, 205 (**2002**).
91. A. M. E. S. Raj, C. M. Magdalane, and K. S. Nagaraja, *Phys. Status Solidi (a)* 191, 230 (**2002**).
92. A. M. E. S. Raj, C. Mallika, K. Swaminathan, O. M. Sreedharan, and K. S. Nagaraja, *Sens. Actuators B* 81, 229 (**2002**).
93. L. G. Wade, Jr., *Organic Chemistry*, Prentice Hall, NJ (**2001**).
94. Y. Sakai, Y. Sadaoka, and M. Matsuguchi, *Sens. Actuators B* 35, 85 (**1996**).
95. K. L. Rauen, D. A. Smith, and W. R. Heineman, *Sens. Actuators B* 17, 61 (**1993**).
96. S. Tsuchitani, T. Sugawara, N. Kinjo, and S. Ohara, *Sens. Actuators* 15, 378 (**1988**).
97. C. W. Lee, H. W. Rhee, and M. S. Gong, *Synth. Metals* 106, 177 (**1999**).
98. M. S. Gong, J. S. Park, M. H. Lee, and H. W. Rhee, *Sens. Actuators B* 86, 160 (**2002**).
99. K. Ogura, H. Shiigi, and M. Nakayama, *J. Electrochem. Soc.* 143, 2925 (**1996**).
100. M. Yang, Y. Li, X. Zhan, and M. Ling, *J. Appl. Polym. Sci.* 74, 2010 (**1999**).
101. K. Sager, G. Gerlach, and A. Schroth, *Sens. Actuators B* 18, 85 (**1994**).
102. N. M. Tashtoush, J. D. N. Cheeke, and N. Eddy, *Sens. Actuators B* 49, 218 (**1998**).
103. B. D. Gupta and Ratnanjali, *Sens. Actuators B* 80, 132 (**2001**).
104. K. Ogura, T. Tonosaki, and H. Shiigi, *J. Electrochem. Soc.* 148, H21 (**2001**).
105. K. L. Rauen, D. A. Smith, W. R. H. Johnson, R. Seguin, and P. Stoughton, *Sens. Actuators B* 17, 61 (**1993**).
106. Y. Sakai, Y. Sadaoka, M. Matsuguchi, and H. Sakai, *Sens. Actuators B* 25, 689 (**1995**).
107. Y. Sakai, M. Matsuguchi, and T. Hurukawa, *Sens. Actuators B* 66, 135 (**2000**).
108. M. S. Gong, M. H. Lee, and H. W. Rhee, *Sens. Actuators B* 73, 185 (**2001**).
109. C. W. Lee, H. W. Rhee, and M. S. Gong, *Sens. Actuators B* 73, 124 (**2001**).
110. S. H. Park, J. S. Park, C. W. Lee, and M. S. Gong, *Sens. Actuators B* 86, 68 (**2002**).
111. M. S. Gong, S. W. Joo, and B. K. Choi, *Sens. Actuators B* 86, 81 (**2002**).
112. M. S. Gong, S. W. Joo, and B. K. Choi, *J. Mater. Chem.* 12, 902 (**2002**).
113. C. W. Lee, Y. Y. Kim, S. W. Joo, and M. S. Gong, *Sens. Actuators B* 88, 21 (**2003**).
114. S. Tsuchitani, T. Sugawara, N. Kinjo, S. Ohara, and T. Tsunoda, *Sens. Actuators* 15, 375 (**1988**).
115. Y. Sakai, M. Matsuguchi, and N. Yonesato, *Electrochim. Acta* 46, 1509 (**2001**).
116. C. W. Lee, O. Y. Kim, and M. S. Gong, *J. Appl. Polym. Sci.* 89, 1062 (**2003**).
117. M. S. Gong, C. W. Lee, S. W. Joo, and B. K. Choi, *J. Mater. Sci.* 37, 4615 (**2002**).
118. S. Y. Son and M. S. Gong, *Sens. Actuators B* 86, 168 (**2002**).
119. I. Palacios, R. Castillo, and R. A. Vargas, *Electrochim. Acta* 48, 2195 (**2003**).
120. A. Y. Coran, *J. Appl. Polym. Sci.* 87, 24 (**2003**).
121. M. Matsuguchi, Y. Sadaoka, Y. Nuwa, M. Shinmoto, Y. Sakai, and T. Kuroiwa, *J. Electrochem. Soc.* 141, 614 (**1994**).
122. M. Matsuguchi, M. Shinmoto, Y. Sadaoka, T. Kuroiw, and Y. Sakai, *Sens. Actuators B* 34, 349 (**1996**).
123. A. G. Macdiarmid, *Synth. Metals* 21, 79 (**1987**).
124. J. Margolis, *Conductive Polymers and Plastics*, Chapman and Hall, NY (**1989**).
125. R. W. Munn, A. Miniewicz, and B. Kuchta, Electrical and Related Properties of Organic Solids, Kluwer Academic Publishers, MA (**1997**).
126. G. Schopf and G. Kobmehl, *Polythiophenes-Electrically Conductive Polymers*, Springer, Berlin (**1997**).
127. E. H. S. Nalwa, *Handbook of Organic Conductive Molecules and Polymers*, Wiley and Sons, NJ (**1997**), Vol. 4.
128. D. Braun and A. J. Heeger, *Appl. Phys. Lett.* 58, 1982 (**1991**).
129. K. West, in *Risø Int. Energy Conference*, Risø, Denmark (**2003**).
130. H. E. Katz, X. M. Hong, A. Dodabalapur, and R. Sarpeshkar, *J. Appl. Phys.* 91, 1572 (**2002**).
131. A. Bearzotti, A. d'Amico, A. Furlani, G. Iucci, and M. V. Russo, *Sens. Actuators B* 9, 451 (**1992**).
132. H. V. Shah, E. L. Hanson, and G. A. Arbuckle-Keil, *J. Electrochem. Soc.* 148, H120 (**2001**).
133. M. Nechtschein, C. Santier, J. P. Travers, J. Chroboczek, A. Alix, and M. Ripert, *Synth. Metals* 18, 311 (**1987**).
134. J. C. Chiang and A. G. MacDiarmid, *Synth. Metals* 13, 193 (**1986**).
135. M. Angelopoulos, A. Ray, and A. G. Mcdiarmid, *Synth. Metals* 21, 21 (**1987**).
136. J. P. Travers and M. Nechtschein, *Synth. Metals* 21, 135 (**1987**).
137. K. Ogura, T. Tonosaki, and H. Shiigi, *J. Electrochem. Soc.* 148, H21 (**2001**).
138. T. Tonosaki, T. Oho, K. Isomura, and K. Ogura, *J. Electroanal. Chem.* 520, 89 (**2002**).
139. K. Ogura, H. Shiigi, M. Nakayama, and A. Ogawa, *J. Polym. Sci.: Part A: Polym. Chem.* 37, 4458 (**1999**).
140. K. Ogura, R. C. Patil, H. Shiigi, T. Tonosaki, and M. Nakayama, *J. Polym. Sci.: Part A: Polym. Chem.* 38, 4343 (**2000**).
141. H. Sun, M. Yang, and M. Ling, *Chinese Chem. Lett.* 11, 1097 (**2000**).
142. Y. Li and M. Yang, *Synth. Metals* 128, 293 (**2002**).
143. Y. Li and M. Yang, *Sens. Actuators B* 85, 73 (**2002**).
144. P. M. Harrey, B. J. Ramsey, P. S. A. Evans, and D. J. Harrison, *Sens. Actuators B* 87, 226 (**2002**).
145. A. R. K. Ralston, C. F. Klein, P. E. Thoma, and D. D. Denton, *Sens. Actuators B* 34, 343 (**1996**).
146. M. Dokmeci and K. Najafi, *J. MEMS* 10, 197 (**2001**).
147. M. Matsuguchi, Y. Sadaoka, K. Nosaka, M. Ishibashi, Y. Sakai, T. Kuroiwa, and A. Ito, *J. Electrochem. Soc.* 140, 825 (**1993**).
148. X. Liu, G. F. Eriksent, and O. Leistikot, *J. Micromech. Microeng.* 5, 147 (**1995**).
149. J. M. Ingram, M. Greb, J. A. Nicholson, and A. W. Fountain, *Sens. Actuators B* 96, 283 (**2003**).
150. H. Grange, C. Beith, H. Boucher, and G. Delapierre, *Sens. Actuators* 12, 291 (**1987**).
151. Y. Sadaoka, M. Matsugucgi, Y. Sakai, and K. Takahashi, *J. Mater. Sci. Lett.* 7, 121 (**1988**).
152. M. Matsuguchi, S. Umeda, Y. Sadaoka, and Y. Sakai, *Sens. Actuators B* 49, 179 (**1998**).
153. M. Matsuguchi, S. Kubo, and Y. Sakai, *Electrochemistry* 67, 170 (**1999**).
154. C. Roman, O. Bodea, N. Prodan, A. Levi, E. Cordosa, and I. Manoviciu, *Sens. Actuators B* 25, 710 (**1995**).
155. J. M. M. Perez and C. Freyre, *Sens. Actuators B* 42, 27 (**1997**).

156. T. Kuroiwa, T. Miyagishi, A. Ito, M. Matsuguchi, Y. Sadaokab, and Y. Sakai, *Sens. Actuators B* 25, 692 **(1995)**.
157. A. Te'telin, C. Pellet, C. Laville, and G. N'Kaoua, *Sens. Actuators B* 91, 211 **(2003)**.
158. F. Kraus, S. Cruz, and J. Muller, *Sens. Actuators B* 88, 300 **(2003)**.
159. A. W. Brewer, B. Cwilong, and G. M. B. Dobson, *Proc. Phys. Soc.* 60, 52 **(1948)**.
160. S. H. Jury, Y. W. Kim, and L. P. Bosanquet, *Anal. Chem.* 39, 912 **(1967)**.
161. M. G. Kovac, D. Chleck, and P. Goodman, *Solid State Technol.* 21, 35 **(1978)**.
162. R. S. Jachowicz, *Sens. Actuators B* 7, 455 **(1992)**.
163. R. S. Jachowicz and W. J. Makulski, *IEEE Trans. Instrum. Measur.* 42, 828 **(1993)**.
164. R. S. Jachowicz and D. Zalewski, *Sens. Actuators A* 42, 503 **(1994)**.
165. Matsumoto and S. Toyooka, *Jpn. J. Appl. Phys. Part 1* 34, 316 **(1995)**.
166. S. Matsumoto and S. Toyooka, *Jpn. J. Appl. Phys. Part 1* 34, 5847 **(1995)**.
167. M. Kimura, *Sens. Actuators B* 33, 156 **(1996)**.
168. F. Pascal-Delannoy, A. Sackda, A. Giani, A. Foucaran, and A. Boyer, *Sens. Actuators A* 65, 165 **(1998)**.
169. B. Sorli, F. Pascal-Delannoy, A. Giani, A. Foucaran, and A. Boyer, *Sens. Actuators A* 100, 24 **(2002)**.
170. Wohltjen, *Anal. Chem.* 51, 1458 **(1979)**.
171. H. Wohltjen, *Sens. Actuators* 5, 307 **(1984)**.
172. J. F. Vetelino, R. Lade, and R. S. Falconer, *IEEE Trans. UFFC* 34, 156 **(1987)**.
173. V. I. Anisimkin, I. M. Kotelyanski, V. I. Fedosov, C. Caliendo, P. Verardi, and E. Verona, in *Proc. IEEE Ultrasonic Symp.*, Seattle, WA **(1995)**.
174. M. D. Ward and D. A. Buttry, *Science* 248, 1000 **(1990)**.
175. H. Kuisma and T. Wiik, U.S. Patent 4,378,168 **(1983)**.
176. D. W. Galipeau, J. D. Stroschine, K. A. Snow, K. A. Vetelino, K. R. Hines, and P. R. Story, *Sens. Actuators B* 25, 696 **(1995)**.
177. M. Hoummady, C. Bonjour, J. Collins, F. Lardet-Vieudrin, and G. Martin, *Sens. Actuators B* 27, 315 **(1995)**.
178. K. A. Vetelino, P. R. Story, R. D. Mileham, and D. W. Galipeau, *Sens. Actuators B* 35, 91 **(1996)**.
179. R. Jachowicz and J. Weremczuk, *Sens. Actuators A* 85, 75 **(2000)**.
180. J. Weremczuk, Z. Gniazdowski, J. M. Lysko, and R. S. Jachowicz, *Sens. Actuators A* 92, 10 **(2001)**.
181. J. Weremczuk, *IEEE Trans. Instrum. Measur.* 51, 1223 **(2002)**.
182. D. Chleck, P. Goodman, and M. G. Kovac, U.S. Patent No. 4,143,177 **(1979)**.
183. R. K. Nahar and V. K. Khanna, *Int. J. Electron.* 52, 557 **(1982)**.
184. V. K. Khanna and R. K. Nahar, *Sens. Actuators* 5, 187 **(1984)**.
185. R. K. Nahar, V. K. Khanna, and W. S. Khokle, *J. Phys. D: Appl. Phys.* 17, 2087 **(1984)**.
186. S. Hasegawa, in *30th Electronic Comp. Conf.*, IEEE, San Francisco, CA **(1980)**.
187. J. C. Harding, Jr., in *Proc. Int. Symp. on Moisture and Humidity*, Washington, DC **(1985)**.
188. K. Suzuki, K. Koyama, T. Inuzuka, and Y. Nabeta, in *Proc. 3rd Sensor Symp.*, IEEE of Japan, Tokyo, Japan **(1983)**.
189. R. S. Alwitt, *J. Electrochem. Soc.* 118, 1730 **(1971)**.
190. System I hygrometer and options, *Operating and Service Manual*, Panametrics Ltd., Shannon, Ireland **(1982)**.
191. Z. Chen and M.-C. Jin, *J. Mater. Sci. Lett.* 11, 1023 **(1992)**.
192. G. P. Wirtz and S. D. Brown, in *Proc. Conf. Coatings and Bimetallics for Aggressive Environments*, Metals Park, OH **(1985)**.
193. K. A. Koshkarian and W. M. Kriven, *J. Phys. Colloq.* 49, C5-213 **(1988)**.
194. S. D. Brown, K. J. Kuna, and T. B. Van, *J. Am. Ceram. Soc.* 54, 384 **(1971)**.
195. L. L. Gruss and W. McNeill, *Electrochem. Technol.* 1, 283 **(1963)**.
196. W. McNeill, *J. Electrochem. Soc.* 105, 544 **(1958)**.